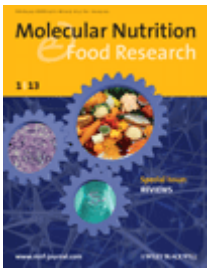

Stilbenoid-mediated epigenetic activation of Semaphorin 3A in breast cancer cells involves changes in dynamic interactions of DNA with DNMT3A and NF1C transcription factor

Journal:	*Molecular Nutrition and Food Research*
Manuscript ID	mnfr.201801386.R1
Wiley - Manuscript type:	Research Article
Date Submitted by the Author:	n/a
Complete List of Authors:	Beetch, Megan ; The University of British Columbia, Food, Nutrition and Health, Faculty of Land and Food Systems Lubecka, Katarzyna; Medical University of Lodz, Department of Biomedical Chemistry Shen, Kate; The University of British Columbia, Food, Nutrition and Health, Faculty of Land and Food Systems Flower, Kirsty; Imperial College London, Epigenetic Unit, Department of Surgery and Cancer Harandi-Sadeh, Sadaf; The University of British Columbia, Food, Nutrition and Health, Faculty of Land and Food Systems Suderman, Matthew; University of Bristol, School of Social and Community Medicine; University of Bristol, MRC Integrative Epidemiology Unit Flanagan, James; Imperial College London, Epigenetic Unit, Department of Surgery and Cancer Stefanska, Barbara; The University of British Columbia, Food, Nutrition and Health, Faculty of Land and Food Systems
Keywords:	DNA methylation, stilbenoids, breast cancer, DNMT3A, NF1C, tumor suppression

GRAPHICAL ABSTRACT

Loci-specific hypermethylation occurring during carcinogenesis is believed to contribute to silencing of key genes regulating cell proliferation and cell function. The present findings show that dietary polyphenols of the stilbenoid class can reverse this process of hypermethylation by modulating dynamics of the interaction of DNA with DNMT3A and NF1C transcription factor at promoters of genes.

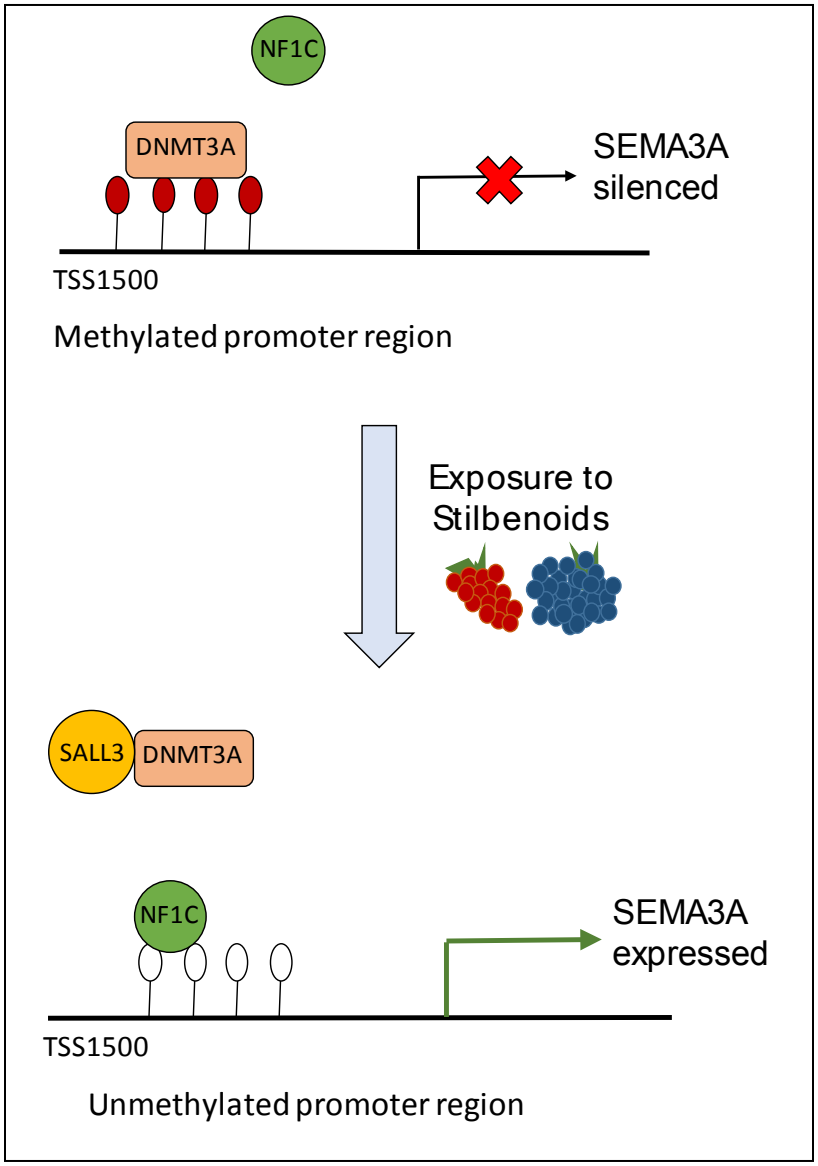

Stilbenoid-mediated epigenetic activation of Semaphorin 3A in breast cancer cells involves changes in dynamic interactions of DNA with DNMT3A and NF1C transcription factor

Megan Beetch[1], Katarzyna Lubecka[2], Kate Shen[1], Kirsty Flower[3], Sadaf Harandi-Zadeh[1], Matthew Suderman[4,5], James M Flanagan[3], and Barbara Stefanska[1]*

[1] Food, Nutrition and Health Program, Faculty of Land and Food Systems, the University of British Columbia, Vancouver, BC, Canada

[2] Department of Biomedical Chemistry, Medical University of Lodz, Lodz, Poland

[3] Epigenetic Unit, Department of Surgery and Cancer, Imperial College London, London, UK

[4] School of Social and Community Medicine, University of Bristol, Bristol, UK

[5] MRC Integrative Epidemiology Unit, University of Bristol, Bristol, UK

Running title: Epigenetic activation of SEMA3A by stilbenoids

Keywords: DNA methylation, stilbenoids, breast cancer, DNMT3A, NF1C, tumor suppression

The Authors declare no conflict of interest.

*To whom correspondence should be addressed:

Dr. Barbara Stefanska

Assistant Professor

Faculty of Land and Food Systems

University of British Columbia

2205 East Mall, FNH 150

Vancouver, BC V6T 1Z4

Phone: +1 604-822-2524, Fax: +1 604-822–5143

barbara.stefanska@ubc.ca

http://www.landfood.ubc.ca/barbara-stefanska/

http://lsi.ubc.ca/person/barbara-stefanska/

ABSTRACT

Scope: Loci-specific increase in DNA methylation occurs in cancer and may underlie gene silencing. We investigate whether dietary stilbenoids, resveratrol and pterostilbene, exert time-dependent effects on DNA methylation patterns and specifically methylation-silenced tumor suppressor genes in breast cancer cells.

Methods and Results: Following genome-wide DNA methylation analysis with Illumina-450K, we identified changes characteristic of early and late response to stilbenoids. Interestingly, often the same genes but at different CpG loci, the same gene families or the same functional gene categories were affected. CpG loci that lost methylation in exposed cells corresponded to genes functionally associated with cancer suppression. There was a group of genes, including *SEMA3A*, at which the magnitude of hypomethylation in response to stilbenoids rises with increasing invasive potential of cancer cells. Decreased DNA methylation at *SEMA3A* promoter and concomitant gene upregulation coincided with increased occupancy of active histone marks. Open chromatin upon exposure to stilbenoids might be linked to decreased DNMT3A binding followed by increased NF1C transcription factor occupancy. Sequestration of DNMT3A is possibly a result of stilbenoid-mediated increase in *SALL3* expression which was previously shown to bind and inhibit DNMT3A activity.

Conclusions: Our findings define mechanistic players in stilbenoid-mediated epigenetic reactivation of genes suppressing cancer.

GRAPHICAL ABSTRACT

Loci-specific hypermethylation occurring during carcinogenesis is believed to contribute to silencing of key genes regulating cell proliferation and cell function. The present findings show that dietary polyphenols of the stilbenoid class can reverse this process of hypermethylation by modulating dynamics of the interaction of DNA with DNMT3A and NF1C transcription factor at promoters of genes.

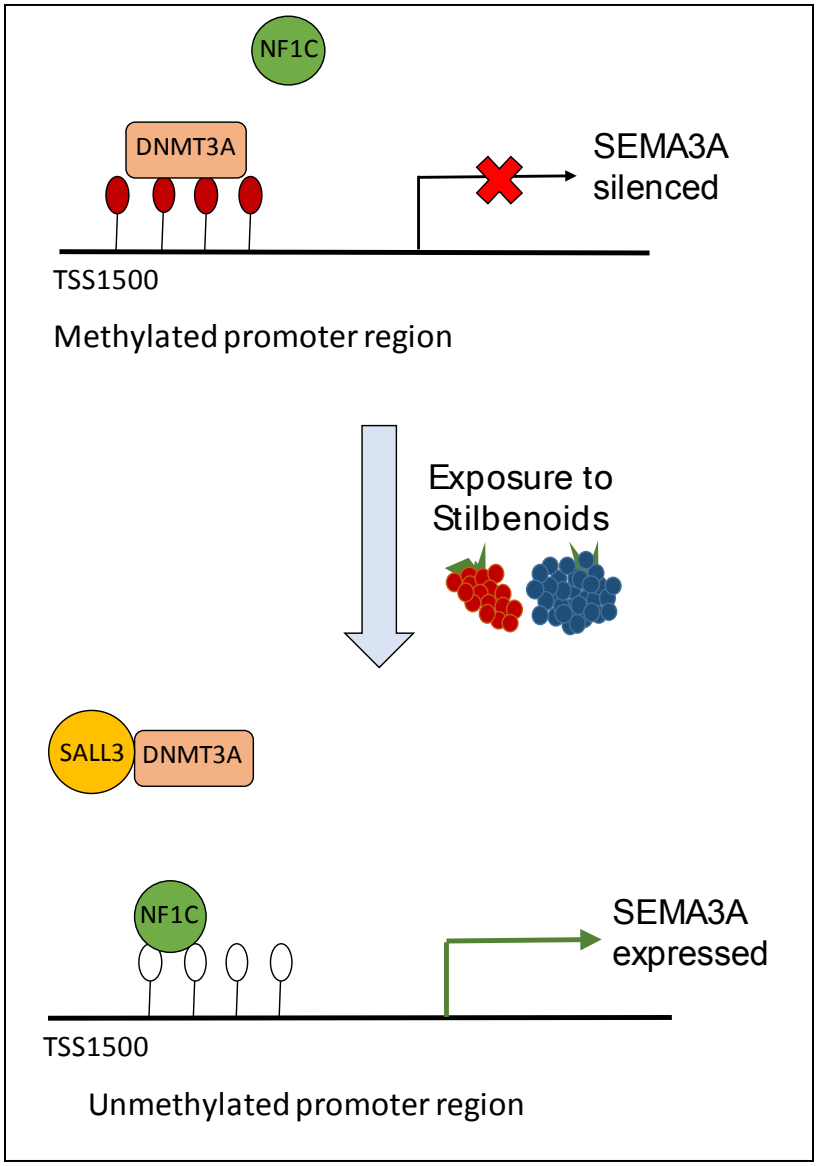

INTRODUCTION

The breast is the leading site of new cancer cases in women [1, 2]. Even more striking, 1 in 8 women in North America will develop breast cancer in her lifetime [1, 2]. Furthermore, 85% of women who are diagnosed with breast cancer have no family history of breast cancer, meaning that the majority of cases are sporadic [1, 2]. Although gender and age are strong predictors of diagnosis, modifiable factors such as environmental exposures and lifestyle factors, including alcohol, smoking, poor diet, physical inactivity, overweight/obesity, appear to play an important role in development of breast cancer, indicating potential role for epigenetics as a driving force of the disease [3].

Epigenetics is the study of heritable gene expression changes that are not due to a change in the DNA sequence. Epigenetic modifications, particularly DNA methylation, have attracted a significant amount of attention for the prevention and treatment of different illnesses with cancer at the forefront, mainly due to the inherent reversibility of epigenetic states [4]. In mammals, DNA methylation occurs mainly on the cytosine of CpG dinucleotide and is catalyzed by DNA methyltransferases (DNMTs). The promoters of approximately 80% of genes contain dense regions of CpGs called CpG islands. In normal cells, these islands are typically unmethylated, allowing expression of the associated gene. In cancer cells, certain CpG islands in gene promoters become hypermethylated [4]. It occurs mostly within tumor suppressor genes (TSGs) leading to their silencing, which can participate in tumor formation. In contrast, promoters of certain genes functionally linked to processes accelerating carcinogenesis become hypomethylated, which leads to their up-regulation and contributes to cancer [5-12]. Thus, reversing alterations in DNA methylation constitutes an excellent anti-cancer approach.

Certain dietary constituents have been shown to exert beneficial effects in cancer, including polyphenols from grapes and blueberries, namely resveratrol (RSV) and its dimethylated analog pterostilbene (PTS) [13-18]. These compounds were shown to have anti-cancer properties, however studies to date have been exploratory and limited without direct mechanistic input [13, 16-19]. Several pieces of evidence indicate that modifying the epigenome, specifically DNA methylation patterns, and subsequently gene expression may be a mediator of anti-cancer effects of dietary polyphenols [20-23]. Previous studies have found that RSV reversed hypermethylation and silencing of several established TSGs such as *BRCA1*, *PTEN*, *APC* and *RARbeta2*, and inhibited breast cancer growth [21, 22, 24]. Although these studies provide proof of principle for targeting hypermethylated TSGs by polyphenols, they are limited to candidate genes and do not address underlying mechanisms.

Our recent genome-wide investigation into DNA methylation patterns demonstrates that loci-specific increases and decreases in DNA methylation occur in breast cancer cells in response to RSV [25]. We specifically described genes that gain methylation and are enriched with oncogenic pathways [25]. In the present study, we extended our investigation by performing Illumina Infinium Human Methylation 450K BeadChip microarray to test time-dependent genome-wide effects and focused on genes that lose methylation upon exposure to RSV and fall into a category of potential TSGs, in lowly invasive MCF10CA1h and highly invasive MCF10CA1a breast cancer cells.

We found changes characteristic of early and late response to RSV, indicating that RSV treatment

often targets for differential methylation the same genes but at different CpG loci, the same gene families or the same functional categories of genes upon 9-day compared with 4-day exposure. Among all genes containing CpG loci hypomethylated upon exposure to stilbenoids, we identified a group of 113 genes that lose methylation in both lowly MCF10CA1h and highly MCF10CA1a invasive breast cancer cells, and are associated with functions attenuating cancerous properties. One of the highest differences was located within *SEMA3A*, a gene found to have a potential tumor suppressor role in breast cancer [26, 27]. DNA hypomethylation of *SEMA3A* promoter as confirmed quantitatively by pyrosequencing coincided with increase in gene expression upon exposure to stilbenoids. Mechanistic studies indicated the presence of DNMT3A binding at *SEMA3A* promoter in cancer cells, which is diminished in response to stilbenoids. Decrease in DNMT3A binding is associated with increased occupancy of NF1C transcription factor, which may contribute to active *SEMA3A* transcription. In addition, we detected increased expression of sal-like 3 (*SALL3*), a negative regulator of DNMT3A activity, upon treatment with stilbenoids [28]. Our results indicate that stilbenoids target specific genes that are hypermethylated and silenced in cancer. Reversal of methylation-mediated silencing of these genes by stilbenoids is potentially linked to anti-cancer properties of these compounds.

MATERIALS AND METHODS

Cell culture and treatment with resveratrol (RSV) and pterostilbene (PTS)

Human mammary epithelial MCF10A cell line and human breast cancer MCF10CA1h and MCF10CA1a cell lines were cultured in DMEM/F12 (1:1) medium (Gibco) supplemented with 5% horse serum (Gibco), 1U/ml penicillin and 1µg/ml streptomycin (Gibco). Medium for

MCF10A cells (ATCC, CRL-10317, USA) was additionally supplemented with 20 ng/ml epidermal growth factor (Sigma-Aldrich, St. Louis, MO, USA), 100 ng/ml cholera toxin (Calbiochem, EMD Millipore, Billerica, MA, USA), 0.01 mg/ml insulin (Sigma-Aldrich, St. Louis, MO, USA), and 500 ng/ml hydrocortisone (Sigma-Aldrich, St. Louis, MO, USA). MCF10CA1h and MCF10CA1a breast cancer cells used in our experiments were derived from tumor xenografts of MCF10A cells transformed with constitutively active Harvey-*ras* oncogene, and represent respectively well- and poorly-differentiated malignant tumors. All cell lines were routinely verified by morphology, invasion and growth rate. Cell lines were authenticated by DNA profiling using the short tandem repeat (ATCC). Cells, grown in a humidified atmosphere of 5% carbon dioxide at 37°C, were treated with resveratrol (RSV, Sigma-Aldrich, St. Louis, MO, USA) or pterostilbene (PTS, Cayman Chem., Ann Arbor, MI, USA) freshly resuspended in ethanol. 24 h prior to treatments, cells were plated at a density of 2-3 x 10^5 followed by exposure to RSV or PTS at 0-20 μM concentrations for 4 days. Cells were then passaged 1:50 and exposed for additional 4 days (9-day exposure).

Illumina Infinium Human Methylation 450K BeadChip microarray

DNA from cells treated with ethanol as a vehicle control and from cells exposed to RSV was isolated using standard phenol:chloroform extraction protocol and subjected to genome-wide DNA methylation analysis using Infinium HumanMethylation 450K BeadChip, as described previously in detail [25]. Hybridization and scanning were performed in the Genomics Facility of University of Chicago, IL. Raw data were processed using the Methylation module (version 1.9.0) of the GenomeStudio software (Illumina; version 2011.1) followed by preprocessing using R Bioconductor minfi package and the analysis of differential methylation in R Bioconductor limma

package. The microarray data for MCF10CA1h cells upon 4-day exposure to RSV are presented in the current manuscript for the first time. The microarray data on hypermethylated genes upon 9-day RSV exposure in both MCF10CA1h and MCF10CA1a breast cancer cell lines were previously reported by our group [25] and re-analyzed in the current manuscript with focus on hypomethylated genes in response to RSV. The microarray data are available from Gene Expression Omnibus [accession numbers: GSE80794 for MCF10CA1h (9-day exposure) and MCF10CA1a (9-day exposure) breast cancer cells; GSE113299 for MCF10A mammary epithelial cells; GSE132670 for MCF10CA1h breast cancer cells (4-day exposure)].

DNA isolation and pyrosequencing

DNA, isolated using standard phenol:chloroform extraction protocol, was treated with sodium bisulfite as previously described [25, 29]. HotStar Taq DNA polymerase (Qiagen) and biotinylated primers were used to amplify bisulfite converted promoter sequences of the selected genes (please see Supplementary Table S1A for primer sequences). Pyrosequencing of the biotinylated DNA strands was performed in the PyroMarkTMQ24 instrument (Qiagen) as previously described [25, 30]. Percentage of methylation at a single CpG site resolution was calculated using PyroMarkTMQ24 software.

RNA isolation and qPCR

TRIzol (Invitrogen) was used to isolate total RNA which served as a template for cDNA synthesis with AMV reverse transcriptase (Roche Diagnostics), according to the manufacturer's protocol. Amplification reaction was performed in CFX96 Touch Real-Time PCR Detection System (Bio-Rad) using 2 µl of cDNA, 400 nM forward and reverse primers (please see Supplementary Table

S1B for sequences), and 10 µl of SsoFast EvaGreen Supermix (Bio-Rad) in a final volume of 20 µl. The following cycles were used in the amplification reaction: denaturation at 95 °C for 10 min, amplification for 60 cycles at 95 °C for 10s, annealing temperature for 10s, 72 °C for 10s, and final extension at 72 °C for 10 min. The CFX Maestro Software (Bio-Rad) was used to quantify gene expression with a standard curve-based analysis. QPCR data is presented as gene of interest/REF. The analysis of the QPCR results was performed according to Pfaffl's method [31, 32], where so-called relative level of expression (relative to geometric mean of expression level of reference genes) is calculated. REF is a reference gene factor consisting of expression of 3 reference genes (GAPDH, RPS17, and 18S). Please see Supplementary Materials for details regarding reference gene factor.

Chromatin immunoprecipitation (ChIP) and qChIP

Chromatin immunoprecipitation was performed as previously described in detail [25, 33, 34]. Briefly, one sub-sample was maintained as an input. The second sub-sample was incubated with anti-acetyl-Histone H3 Lys9 rabbit antibody (H3K9ac, Millipore, 07-352), anti-trimethyl-Histone H3 Lys27 rabbit antibody (H3K27me3, Millipore, 07-449), anti-DNA methyltransferase 3A rabbit antibody (DNMT3A, Abcam ab2850), and anti-nuclear factor 1/C rabbit antibody (NF1C, Millipore Sigma ABE1387). The third sub-sample was incubated with rabbit IgG non-specific antibody (negative control, Santa-Cruz Biotechnology, sc-2027). Fraction of DNA bound to antibodies was washed, eluted and used as a template for QPCR (qChIP). 25ng of input, antibody bound and IgG bound DNA was used as starting material in all conditions. Levels of H3K9ac, H3K27me3, DNMT3A, and NF1C binding were expressed as (Bound-IgG)/Input. Primers used in qChIP are listed in Supplementary Table S1B.

Cell transfection with siRNA

MCF10CA1a cells were plated at a density of 4 $\times 10^5$ per 10-cm tissue culture dish, 24 h prior to treatment with small interfering RNAs (siRNAs). All siRNA sequences were obtained from Dharmacon, including control siRNA (siCtrl) and human DNMT3A siRNA (siDNMT3A) (see Supplementary Table S1C for sequences). The cells were transfected with siRNA using Lipofectamine RNAiMAX (Invitrogen, Carlsbad, CA). A concentration of 56 nM was used for all siRNAs, which was determined as optimal in our previous studies [5]. Please see Supplementary Materials for details on transfection procedure.

Statistical analysis

Human Methylation 450K microarray data were pre-processed using GenomeStudio and IMA (Illumina Methylation Analyzer for 450K, R/Bioconductor), including quality control, background correction, normalization, probe scaling, and adjustment for batch effect. Linear modelling in R Bioconductor package limma was applied to calculate differential methylation between sample groups. Limma uses an empirical Bayes moderated t-test, computed for each probe, with standard errors moderated using information from the full set of probes [35]. Probes with a methylation difference of beta value greater than 0.05 (5%) and with moderated t-test $P<0.05$ were considered as statistically significant.

Unpaired *t*-test with two-tailed distribution was used for statistical analysis of pyrosequencing, QPCR, qChIP, and cell growth assays. Each value represents the mean ± S.D. of three independent experiments. The results were considered statistically significant when $P < 0.05$.

RESULTS

Resveratrol (RSV) and pterostilbene (PTS) decrease breast cancer cell growth and invasive properties

In order to examine the effects of increasing concentrations of stilbenoid compounds, RSV and PTS, on the number of viable and dead cells, we used trypan blue exclusion test. Breast cancer cells, MCF10CA1h and MCF10CA1a, as well as MCF10A mammary epithelial cells, used as a normal cell model, were treated with RSV or PTS at 0-20μM concentrations for 4 or 9 days to determine time- and concentration-dependent effects on cell growth. MCF10CA1h and MCF10CA1a cells are derived from mice xenografts of MCF10A-*ras* cells that were generated by transfecting MCF10A mammary epithelial cells with constitutively active T24 Harvey-*ras* oncogene. MCF10CA1h and MCF10CA1a cells form well-differentiated and poorly differentiated tumors in xenograft models, respectively. Thus, MCF10CA1h cells have low invasive properties, whereas MCF10CA1a cells have characteristics of highly invasive cancer phenotype. This isogenic cell model appears to be attractive for studying epigenetic effects that arise during breast carcinogenesis without genetic differences as a confounding factor.

Stilbenoid treatment of MCF10CA1h and MCF10CA1a breast cancer cells resulted in significant inhibition of cell growth compared to cells treated with ethanol as a vehicle control (Supplementary Figure S1A and S1B). These effects were dose- and time-dependent in both breast cancer cell lines treated with RSV or PTS. The compounds caused approximately 50% decrease in cell number (IC_{50}) at doses of 15μM for RSV and 7μM for PTS on day 9-exposure (Supplementary Figure S1A and S1B), which confirms our previous findings [25]. At the same

time, the number of dead cells did not exceed 10% indicating non-cytotoxic mode of action at these concentrations (Supplementary Figure S1C). In accordance with what we previously reported, invasive capacity and anchorage independent growth were attenuated by 15μM RSV and 7μM PTS (Supplementary Figure S1D and S1E). Additionally, these doses did not cause significant differences in cell number in MCF10A mammary epithelial cells (Supplementary Figure S1F). For these reasons, doses of 15μM for RSV and 7μM for PTS were chosen for further experiments.

Exposure to resveratrol (RSV) leads to time-dependent genome-wide changes in the DNA methylation patterns in breast cancer cells

Using the Illumina Infinium Human Methylation 450K BeadChip microarray, we delineated the DNA methylation patterns upon 4-day and 9-day exposure of MCF10CA1h breast cancer cells to 15μM RSV. We identified 364 hypomethylated CpG sites at day 4 of RSV treatment compared to 990 hypomethylated CpG sites at day 9 of treatment ($P < 0.05$, limma *t*-test) (Figure 1A). While the number of hypomethylated loci increased after longer exposure, the opposite occurred for hypermethylated loci (Figure 1A). Although the number of differentially methylated CpG sites varied between 4- and 9-day treatment, similar genes and gene families were affected in terms of biological functions.

Time-dependent hypermethylation in response to RSV treatment

Functional analysis of genes corresponding to hypermethylated CpG loci upon 4-day RSV exposure revealed important players, silencing of which could at least partially contribute to anti-cancer effects of RSV. We identified genes from the WNT (*WNT16*, *WNT7A*) and NOTCH

(*NOTCH3*, *NOTCH4*) oncogenic signaling pathways, transcriptional regulators of gene expression (*JMJD1C*, *POU1F1*, *POU3F2*, *PRDM16*), genes regulating cell adhesion and migration (*MMP28*, *PTPRN2*), brain-specific genes (several SNORD members of small nucleolar RNAs, *GRIA4*, *MYT1L*), pluripotency genes (*NANOG*, *TCF15*), and serine/threonine protein kinase *ACVR1C*. The latter phosphorylates cytoplasmic SMAD transcription factors facilitating their translocation to the nucleus where SMADs regulate transcription of genes associated with differentiation, growth and apoptosis. RSV-mediated increase in methylation of the genes described above could potentially decrease their expression and consequently attenuate cancerous properties of cells.

We found 299 genes which were hypermethylated at exactly the same CpG positions at both time points of exposure ($P < 9x10\text{-}124$, Fisher's exact test). Additional 637 genes were identified where hypermethylation occurred at different loci on day 4 as compared with day 9 of treatment. Interestingly, 9-day RSV exposure often targeted different CpG loci within the same gene, the same gene family or the same functional gene category, as compared with a short-term exposure (Figure 1B). For instance, among overlapped genes, we detected hypermethylation within members of WNT (*WNT11*, *WNT5A*) and NOTCH (*NOTCH4*) signaling pathways, within metalloproteinase family (*MMP12*), SNORD members of small nucleolar RNAs, *PRDM16* and other members of PRDM family of transcription factors, and serine/threonine protein kinase *ACVR1*. *JMJD1C* was hypermethylated at exactly the same CpG locus on day 4 and day 9, showing a time-dependent increase in methylation and becoming the most robustly hypermethylated gene on day 9 of RSV treatment. *JMJD1C* is a histone demethylase that regulates activity of many transcription factors and has a potential oncogenic role in cancer [36]. Another interesting example is protein tyrosine phosphatase *PTPRN2* which was hypermethylated at different loci on day 4

compared with day 9 of RSV exposure. *PTPRN2* regulates localization of cofilin and phosphatidylinositol 4,5-diphosphate level in the plasma membrane impacting actin dynamics related to cell migration and metastasis. Indeed, *PTPRN2* was shown to promote metastatic breast cancer cell migration [37]. There were also changes characteristic of only 9-day exposure. Additional activators of oncogenic signaling pathways were hypermethylated including Hedgehog (*GLI2*), MAPK (*MAPK12*), and mTOR (*RPS6KA3*, *RPTOR*). We also found additional well established oncogenes among hypermethylated genes such as *BRAF* from Ras/Raf oncogenic signal transduction and *TERT* that maintains telomere ends delaying programmed cell death. Many members of calcium ion channels family *CACNA* that regulate cellular functions, including mitogenesis, proliferation, differentiation, apoptosis and metastasis were hypermethylated on day 9 of RSV treatment.

Time-dependent hypomethylation in response to RSV treatment

Genes encompassing CpG sites hypomethylated upon RSV treatment on day 4 were functionally linked to pathways and processes that inhibit cancer development suggesting their potentially tumor suppressive role. We identified *LIFR* cytokine receptor that inhibits cancer and suppresses metastasis [38], *CSMD1* whose loss contributes to high proliferation, migration and invasion of breast cancer cells [39], *PAX9* transcription factor whose suppression is linked to cancer development, G protein-coupled receptors (GPCRs) from LPHN family (*LPHN1*, *LPHN3*) regulating cell adhesion and frequently inhibited in cancer [40], cadherins *CDH13* and *CDH18* promoting cell adhesion, imprinted gene *PEG3* that induces apoptosis and possesses a tumor suppressing role in glioma [41], and *BRMS1* that promotes binding of histone deacetylase HDAC1 to gene promoters followed by transcriptional inhibition of pro-metastatic genes [42]. *PBRM1* and

PHF20 that are negative regulators of cell proliferation and invasion were also among hypomethylated genes on day 4 [43]. Both *PBRM1* and *PHF20* are involved in epigenetic regulation of gene transcription. *PBRM1* is a subunit of chromatin remodeling complexes while methyllysine-binding protein *PHF20* is a component of the MOF histone acetyltransferase protein complex and is involved in acetylation of histone H4. Interestingly, among RSV hypomethylated genes we found other epigenetic regulators such as *SMARCA4*, *MLL5*, *HDAC5*, and *CDKN2BAS*. *SMARCA4* is part of the large ATP-dependent chromatin remodeling complex SNF/SWI, which is required for transcriptional activation. Similarly, lysine methyltransferase *MLL5* is associated with activation of gene transcription upon methylation of histone H4 and is implicated in regulation of cell cycle progression [44]. On the other hand, histone deacetylase *HDAC5* and *CDKN2BAS* are responsible for gene silencing. *HDAC5* promotes condensed chromatin structure by decrease in acetylation at histone proteins while *CDKN2BAS* encodes functional RNA molecule that interacts with polycomb repressive complexes (PRCs) leading to epigenetic silencing of target genes.

A comparison of 4-day vs. 9-day treatment shows that RSV treatment often targets for hypomethylation the same genes but at different CpG loci, the same gene families or the same functional categories of genes at both time points, which was earlier noted for hypermethylated genes (Figure 1B). Altogether 28 genes, including 15 genes with the same location of hypomethylated loci, overlapped between both treatments ($P < 1x10\text{-}14$, Fisher's exact test). For instance, cell adhesion promoter *LPHN3*, lysine methyltransferase *MLL5*, and long non-coding RNA *CDKN2BAS* were hypomethylated at exactly the same site at 4- and 9-day treatment. Tumor suppressor *CSMD1*, and cadherins *CDH13* and *CDH18* were hypomethylated on day 9 at different CpG loci compared with day 4. *PHF* family of genes regulating histone acetylation and HDAC

family of histone deacetylases were found to be hypomethylated upon 9-day exposure however different members of the families were targeted compared with 4-day treatment. In addition to epigenetic regulators mentioned above (i.e., *PHF*, *HDAC*, *MLL5*, *CDKN2BAS*), we identified *MBD4* and *SUV39H1* among hypomethylated genes that were affected specifically on day 9. *MBD4* is a methyl-CpG binding domain protein and has thymine glycosylase activity important for G:T mismatches. Methylated cytidine in CpG dinucleotides can be deaminated to thymidine that is then excised by MBD4 resulting in DNA demethylation. *SUV39H1* is a histone modifying enzyme with methyltransferase activity specifically for trimethylation of Lys-9 of histone H3 which recruits HP1 proteins and leads to transcriptional repression. Genes implicated in RNA maturation and epigenetic regulation of RNA, such as pre-mRNA alternative splicing regulator *BRUNOL4* and RNA methyltransferase *METTL3*, were also specific to 9-day exposure. In addition, 9-day exposure resulted in hypomethylation of known tumor suppressor genes, *BRCA2* and *HOXA9*.

RSV-mediated loci-specific hypomethylation in lowly and highly invasive breast cancer cells

Next, we compared DNA methylation changes in response to 9-day treatment with 15μM RSV in lowly invasive MCF10CA1h to highly invasive MCF10CA1a breast cancer cells. We previously described genes containing CpG sites that are hypermethylated in response to RSV in both cell lines [25]. In the present study, we focus on CpG sites that are hypomethylated in cells treated with RSV to deliver mechanistic input on diet-mediated epigenetic activation of genes (diff. methylation $\leq$ -0.05, $P < 0.05$, limma *t*-test). Genes hypomethylated in response to RSV would be expected to become expressed and contribute to anti-cancer effects of dietary stilbenoids. Similar amount of hypomethylated CpG sites were detected after RSV treatment in both breast cancer cell

lines (Figure 1C). The magnitude of average hypomethylation across all hypomethylated sites reached approximately -0.25 (delta beta) in MCF10CA1a cells compared to maximum magnitude of hypomethylation of less than -0.20 in MCF10CA1h cells (Figure 1D). More specifically, the majority of CpG sites with the most robust hypomethylation in MCF10CA1a cells showed lower extent of changes in MCF10CA1h cells, demonstrating a stronger effect of RSV in highly invasive breast cancer cells (Table 1). The loci listed in Table 1 are located in gene regulatory regions, including promoters and 5'UTRs of *AGTPBP1*, *SEMA3A*, *FOXN3*, *UACA*, *FAM49A*, *TMEM91*, *CSMD1*, *WFDC3*, *EPN2*, and *HIST1H2BK*. Interestingly, *SEMA3A*, *FOXN3*, and *CSMD1* were shown to be implicated in regulation of invasiveness of cancer cells. Increased expression of *SEMA3A* lowered the ability of cancer cells to invade through extracellular matrix [45] while loss of *FOXN3* promoted growth and migration of cancer cells [46]. In addition, breast cancer patients with low levels of *CSMD1* showed a significantly shorter overall survival [47].

In order to identify loci with the highest probability to be specifically targeted by RSV in breast cancer, we searched for overlap between CpG sites and genes hypomethylated in MCF10CA1h and MCF10CA1a breast cancer cells (Figure 1E). We found 116 CpG sites hypomethylated in response to RSV in both cell lines (Supplementary Table S2) ($P < 4x10\text{-}150$, Fisher's exact test). The majority of these CpG sites were lowly methylated in MCF10A mammary epithelial cells and were gaining high levels of methylation in breast cancer cells (Figure 1F), which could suggest methylation-mediated silencing of corresponding genes in cancer. Exposure to RSV resulted in a similar degree of hypomethylation across all the sites without substantial differences between lowly and highly invasive cells (Figure 1G). Loci whose initial methylation level was higher than 0.3 in MCF10A mammary epithelial cells were coming back to normal levels upon RSV exposure

in both cancer cell lines (Figure 1G).

Out of 116 common CpG sites, 75 were assigned to genes. Additional 38 genes were identified to be hypomethylated in both cell lines although different CpG locus was affected in response to RSV (Supplementary Table S3). The 113 genes identified from the overlap would be considered as strongest targets of RSV and their appearance in both breast cancer cell lines would limit the possibility of cell line-specific artifact. We refer to these genes as "hypomethylated RSV targets". Biological function and signaling pathway analysis for "hypomethylated RSV targets" revealed that the majority of these genes are implicated in increase in cell adhesion, apoptosis, and cell cycle arrest, in regulation of gene transcription and p53 signaling, and in inhibition of WNT oncogenic pathway; functions that indicate tumor suppressive roles of these genes (Figure 1H and 1I). "Hypomethylated RSV targets" include inhibitors of cell migration and invasion such as *CSMD1*, cadherin *CDH6*, and G protein-coupled receptor *LPHN3*. Epigenetic regulators such as *CDKN2BAS* and *METTL3*, and potential tumor suppressors *SEMA3A* and *WFDC3* are also present among 113 "hypomethylated RSV targets". *RBPJ* is another important candidate present among genes hypomethylated in both cancer cell lines. *RBPJ* acts as a transcriptional repressor by recruitment of chromatin remodeling complexes which consequently suppresses oncogenic NOTCH signaling [48].

Tumor suppressor gene *SEMA3A* is epigenetically activated upon exposure to resveratrol (RSV) or pterostilbene (PTS) in breast cancer cells

Our genome-wide DNA methylation analysis of breast cancer cells treated with 15μM RSV revealed a group of genes containing CpG loci at which the magnitude of hypomethylation in

response to stilbenoids rises with increasing invasive potential of cancer cells (Figure 2A). Methylation levels at five out of these CpG sites corresponding to *SEMA3A*, *UACA*, *FAM49A*, *TMEM91*, and *EPN2* were quantitatively measured by pyrosequencing in highly invasive MCF10CA1a breast cancer cells exposed to RSV (Figure 2B). The exact location of the CpG loci is visualized in the gene map in Figure 2B with the tested region blue shaded. Fragments tested in pyrosequencing encompassed a CpG site covered on Illumina (marked in square in Figure 2B) and neighboring CpG loci so that a broader region was investigated. Pyrosequencing confirmed 10-20% hypomethylation within sites located in promoters of *SEMA3A*, *TMEM91*, and *EPN2*, and within gene body of *UACA* and *FAM49A* (Figure 2B, right panel). One of the five genes, *SEMA3A*, was previously shown to exert a tumor suppressor function in breast cancer. One study reported that *SEMA3A* regulates phosphorylation of phosphatase and tensin homolog (PTEN), which in turn activates a chain of tumor suppressor genes to inhibit breast cancer growth, invasiveness and angiogenic capacity [26]. Another study demonstrated a role for *SEMA3A* in proliferative control of tumor-associated macrophages [27]. Silencing of *SEMA3A* in many types of cancer, including breast cancer, was found in publicly available gene expression data in clinical samples, which further supports a tumor suppressor role of *SEMA3A* (Figure 3A). Using publicly available methylation datasets of breast cancer patients, we also confirmed hypermethylation of *SEMA3A* promoter region in tumors at the same CpG locus as the site affected by RSV (Figure 3B, the locus marked in square). *SEMA3A* hypermethylation could at least partly explain downregulation of the gene observed in tumors versus normal tissue. Taken together, this evidence indicates that *SEMA3A* may act as a tumor suppressor regulated by DNA methylation, however epigenetic regulation of *SEMA3A* has not yet been explored. We therefore selected *SEMA3A* for further studies on mechanisms associated with hypomethylation mediated by stilbenoids.

Exposure of MCF10CA1a breast cancer cells to another stilbenoid compound, pterostilbene (PTS), led to hypomethylation of *SEMA3A* promoter at the same RSV target site (Figure 3C). Decrease in *SEMA3A* methylation was linked to increase in gene expression in response to both RSV (1.7-fold increase) and PTS (3.2-fold increase) (Figure 3D), which further supports epigenetic regulation of transcriptional activity of *SEMA3A*. Importantly, although the microarray indicated just slight hypomethylation at the studied CpG site (cg05081033) within *SEMA3A* promoter in lowly invasive MCF10CA1h cells, we detected statistically significant 25% hypomethylation using a quantitative pyrosequencing technique and confirmed 2.3-fold gene upregulation in response to RSV (Figure 3E and 3F), which was comparable with effects detected in MCF10CA1a cells. This further strengthens the role for DNA methylation in regulation of *SEMA3A* expression.

Decreased DNMT3A occupancy within *SEMA3A* promoter in response to resveratrol (RSV) or pterostilbene (PTS)

After validation of DNA hypomethylation and increased expression of *SEMA3A* upon stilbenoid treatment, we sought to delve into the mechanism underlying these effects. As the magnitude of changes in the DNA methylation patterns in response to stilbenoids was higher in highly invasive than in lowly invasive cells, we proceed with highly invasive MCF10CA1a cell line as an experimental model in further investigations. DNA methyltransferases (DNMTs) are enzymes that catalyze the transfer of a methyl group to the 5th position of the cytosine ring on the DNA; thereby they are central players in the DNA methylation reaction. While DNMT1 is mainly responsible for maintenance of the DNA methylation patterns during replication, DNMT3A and DNMT3B are categorized as *de novo* methyltransferases [4]. We found that treatment of

MCF10CA1a breast cancer cells with RSV or PTS caused a reduction of *DNMT3A* expression (Figure 4A). DNMT3A binding at the hypomethylated CpG site within the *SEMA3A* promoter was diminished upon RSV or PTS treatment (Figure 4B). Reduction in *DNMT3A* expression and DNMT3A occupancy at the *SEMA3A* promoter in response to stilbenoids suggests a connection between loss of DNMT3A and hypomethylation. In addition to hypomethylation and lower occupancy of DNMT3A, we observed increased enrichment of active histone mark, acetylation of histone H3 lysine 9 (H3K9ac), and decreased enrichment of repressive histone mark, trimethylation of histone H3 lysine 27 (H3K27me3). Such changes in occupancy of histone modifications are indicative of open chromatin structure and increased transcriptional activity of *SEMA3A* upon exposure to RSV or PTS (Figure 4C and 4D).

DNMT3A knockdown mimics the effects of stilbenoid compounds on DNA methylation and expression of _SEMA3A_

Observed hypomethylation of *SEMA3A* with concomitant decrease in DNMT3A binding to *SEMA3A* promoter in response to stilbenoids suggests the mechanistic involvement of DNMT3A in *SEMA3A* epigenetic regulation. To further test this hypothesis, we depleted the *DNMT3A* gene in MCF10CA1a breast cancer cells using small interfering RNAs (siRNAs). MCF10CA1a cells were transfected with one of four siRNAs targeting DNMT3A (siDNMT3A #1-4) or control siRNA (siCtrl). Measurement of cell growth revealed that all DNMT3A siRNAs led to robust reduction in cell growth after 3 rounds of transfection (Figure 4E). Expression of *DNMT3A* was decreased most effectively by siDNMT3A #1 and siDNMT3A #3 (Figure 4F), therefore we performed further experiments using those DNMT3A siRNAs. Upon *DNMT3A* depletion, expression of *SEMA3A* was significantly increased by 1.5-2 fold (Figure 4G), mimicking the effect

of stilbenoids (Figure 3D). In addition, *DNMT3A* knockdown resulted in a 12% decrease in DNA methylation (Figure 5H) at the same CpG site identified and validated as hypomethylated in response to RSV and PTS treatments (Figure 2B and 3C). These findings suggest that DNMT3A is involved in methylation and silencing of *SEMA3A* in MCF10CA1a cells, providing additional support for DNMT3A as an important mechanistic player in epigenetic activation of *SEMA3A* in response to RSV or PTS.

Nuclear factor 1C (NF1C) occupancy at *SEMA3A* promoter increases upon resveratrol (RSV) and pterostilbene (PTS) treatment

Changes in DNA methylation are known to affect binding of transcription factors to a gene regulatory region [49]. We used TransFac to compute putative transcription factor binding elements encompassing the hypomethylated CpG site in *SEMA3A* promoter. We found several candidates including nuclear factor 1C (NF1C). A response element for NF1C was further found in 80% of hypomethylated loci within "hypomethylated RSV targets", a group of genes hypomethylated in both MCF10CA1h and MCF10CA1a cells (Supplementary Table S3). Additionally, transcription factors from NF1 family have been implicated as key epigenetic regulators in cancer possibly through regulating chromatin accessibility [50]. NF1C was specifically reported to have a tumor suppressor role in breast cancer [51]. For these reasons, we proceeded with experimentally testing whether stilbenoid-mediated changes in DNA methylation near predicted NF1C binding site within the *SEMA3A* promoter affected binding of this potentially important transcription factor. Interestingly, we found that RSV or PTS treatment of highly invasive MCF10CA1a breast cancer cells increased occupancy of NF1C at the *SEMA3A* promoter (Figure 5A). This enrichment in binding was accompanied by a slight 11% increase of *NF1C*

expression in PTS-treated breast cancer cells, while expression of *NF1C* was unchanged in response to RSV (Figure 5B). Such changes in NF1C expression and binding suggest that increased binding of the transcription factor is linked to structural changes in the chromatin state at *SEMA3A* promoter, facilitating DNA-NF1C interaction rather than just a result of increased pool of NF1C available for binding.

DNMT3A inhibitor *SALL3* is upregulated upon stilbenoid treatment

To introduce an upstream element to the proposed mechanism of stilbenoid-mediated epigenetic reactivation of *SEMA3A*, we identified a protein called sal-like 3 (SALL3) that has been reported to directly inhibit DNMT3A activity and impose subsequent DNA hypomethylation [28]. We found that *SALL3* expression was significantly increased by 2.5- and 1.5-fold upon 9-day treatment of MCF10CA1a cells with 15μM RSV or 7μM PTS, respectively (Figure 5C). While further work is needed to confirm SALL3 as a player in this mechanism, the upregulation of this gene may be related to decreased DNMT3A activity by direct binding which consequently results in DNA hypomethylation at the *SEMA3A* promoter (Figure 5D). We propose a mechanism wherein stilbenoid treatment of breast cancer cells results in sequestration of DNMT3A via direct inhibition by SALL3 followed by subsequent DNA hypomethylation at the *SEMA3A* promoter. Decreased methylation at the *SEMA3A* promoter allows NF1C transcription factor to bind and promote a transcriptionally active state (Figure 5D).

DISCUSSION

Functions of tumor suppressor genes (TSGs) are commonly lost during the course of cancer development which is often associated with inactivating mutations or epigenetic silencing [4]. The

latter phenomenon plays an important role in majority of cancer cases without family history. Transcriptionally silenced TSGs as a result of epigenetic alterations, specifically increased DNA methylation within gene regulatory regions, have been shown as a hallmark of cancer [4]. Epigenetic drugs such as DNA methyltransferase inhibitors (DNMTi) target DNMTs to lead to passive DNA hypomethylation with the goal to re-express TSGs that have been silenced by DNA methylation in cancer [4]. However, the effects of DNMTi such as decitabine (5-aza-2'-deoxycytidine) are non-specific which may lead to activation of other genes responsible for side-effects or resistance to therapy. Indeed, the initial patterns of gene expression in patients treated with decitabine may influence the efficacy of this drug. For example, patients with low levels of lysine methyltransferase *MLL5* were developing resistance to low-doses of decitabine [52]. In addition, expression levels of two enzymes involved in decitibine metabolism, namely cytidine deaminase (CDA) and deoxycytidine kinase (DCK), differ between non-responders and responders [53]. Hence, alternative more specific methods of reactivating epigenetically-silenced tumor suppressor genes are needed. As DNA methylation is responsive to environmental stimuli [4], dietary compounds could possibly comprise a novel approach in anti-cancer epigenetic strategies. A genome-wide DNA methylation study where curcumin, a bioactive compound from a spice Turmeric, was compared with decitabine, shows that curcumin caused loci-specific both hyper- and hypomethylation, predominantly in partially-methylated CpG sites, while decitabine treatment led to non-selective hypomethylation [54]. This evidence opens the door to investigating whether other dietary polyphenols can exert specific epigenetic effects and what mechanisms are involved in such an action.

Herein, we were investigating polyphenols from stilbenoid class, such as resveratrol (RSV) and its

natural dimethylated analog pterostilbene (PTS), and their epigenetic effects in breast cancer cells. Stilbenoids were shown to exert anti-cancer effects in cell lines and *in vivo* models however without a clear molecular mechanism demonstrated [13, 16-18]. There are a few reports by us and others on the involvement of epigenetics and specifically DNA methylation in the action of stilbenoids [21, 22, 24, 25, 55, 56]. Briefly, RSV treatment reversed methylation-mediated silencing of TSGs, *BRCA1*, *PTEN*, *APC*, and *RARbeta2*, in breast cancer [21, 22, 24]. Furthermore, both RSV and PTS were shown to increase methylation at specific CpG loci located in pro-inflammatory cytokines and fatty acid synthase gene, respectively, which resulted in gene suppression [55, 56]. In our recent genome-wide study using methylation microarray technology, we further confirmed hyper- and hypomethylation upon treatment with stilbenoids and epigenetic silencing of oncogenic pathways in response to the compounds [25]. Our results confirm what was observed for curcumin [54] and clearly suggest a bidirectional mode of epigenetic effects, whereby the compounds induce DNA hypomethylation and activation of TSGs, with simultaneous DNA hypermethylation and silencing of oncogenes.

In our present study, we demonstrate that stilbenoids at non-cytotoxic concentrations slow down growth of cancer cells by 50% (Supplementary Figure S1) and change DNA methylation patterns causing remodeling rather than robust turn on/off changes on day 4 and day 9 of treatment (Figure 1). Interestingly, similar effects are observed at both time points where often the same genes but at different CpG loci, the same gene families or the same functional categories of genes are differentially methylated (Figure 1B). One excellent example of targeted genes are those involved in epigenetic regulation of gene transcription. For instance, histone demethylase *JMJD1C* with potential oncogenic role [36] is hypermethylated by RSV which would indicate potential

repression of this oncogene. A methyllysine-binding protein family of *PHF* genes encoding for components of the MOF histone acetyltransferase protein complex, lysine methyltransferase *MLL5*, and long non-coding RNA *CDKN2BAS* are involved in epigenetic regulation of gene transcription and become hypomethylated and potentially activated in response to RSV upon 4-day and 9-day exposure (Figure 1B). Additional epigenetic enzymes are affected after 9-day treatment, including *MBD4*, *SUV39H1*, and *METTL3*, which modify DNA, histones, and RNA, respectively. Hence, stilbenoids may exert a very broad effect on transcription of other genes through these epigenetic regulators.

Importantly, although a general finding from the genome-wide analyses is that RSV-hypomethylated genes have a tumor suppressor role and RSV-hypermethylated genes are linked to oncogenic and pro-metastatic functions, there are some in each group that could be functionally categorized the opposite direction. For instance, hypermethylated *SERPINB12* protease inhibitor, located in the serpin gene cluster on chromosome 18, is down-regulated in clinical samples which suggests its potential tumor suppressor role [57]. Hypermethylated *ITGA7* belongs to the integrin family and is a newly identified tumor suppressor gene that decreases migration and invasion of cancer cells [58, 59]. On the other hand, hypomethylated *MMP1* is a potent oncogene promoting metastasis and multi-drug resistance [60, 61], and hypomethylated *PLEKHA5* facilitates metastasis to the brain [62]. Hence, the functional role of differential methylation within those genes in response to RSV is unclear. Several steps could be taken to understand the observed changes. The location of the CpG locus should be closely investigated to establish regulatory role of the region, DNA methylation at surrounding loci should be quantified to evaluate the entire region, and expression of genes in question should be measured to confirm the changes in DNA methylation

are biologically relevant and impact transcriptional activity.

We further compared patterns of changes in DNA methylation in response to RSV in lowly and highly invasive breast cancer cells. We found a group of 113 genes that were hypomethylated in both cancer cell lines. Interestingly, the basal methylation level at CpG loci located in these genes was low in MCF10A mammary epithelial cells (Figure 1F). It would suggest that the genes are expressed in normal cells and become silenced during carcinogenesis through gain of methylation. This would indicate their tumor suppressor role in cancer. Indeed, the genes are involved in inhibition of main pathways associated with oncogenic properties (Figure 1H and 1I) [39, 40, 45, 48, 63]. Among genes that were the most robustly hypomethylated in invasive MCF10CA1a cells, we observed a progressive RSV-mediated hypomethylation from lowly invasive to highly invasive stages (Table 1, Figure 2A). One of the highest changes was identified within a promoter region of *SEMA3A*, a gene with reported tumor suppressor functions (Table 1, Figure 2B) [26, 27]. Publicly available clinical data show methylation of the studied CpG locus within *SEMA3A* and gene downregulation in tumors vs. normal tissue. In our study, the same locus loses methylation upon exposure to RSV which could at least partially be associated with observed increase in *SEMA3A* expression (Figure 3). Importantly, similar effects are observed upon treatment with another stilbenoid, PTS, which is an analog of RSV abundantly present in blueberries (Figure 3). The latter compound is of high interest in future studies due to its high bioavailability compared with RSV which is reflected in a much lower dose of PTS needed to inhibit cancer cell proliferation (Supplementary Figure S1). High PTS bioavailability is likely linked to its chemical structure and slower conversion rate to metabolites [64].

Although activation of methylation-silenced TSGs in response to dietary polyphenols was reported before [20-25], mechanistic studies investigating players involved in this phenomenon are lacking. We therefore elucidated the effects of stilbenoids on gene-protein interactions at *SEMA3A* promoter to enhance our knowledge on epigenetic enzymes, transcription factors and other proteins involved in epigenetic effects imposed by stilbenoid compounds. Among DNA methylating enzymes, DNMTs, we found downregulation of *DNMT3A* leading us to a hypothesis that DNMT3A may be implicated in stilbenoid-mediated loss of methylation at *SEMA3A* promoter (Figure 4A). Indeed, decrease in DNMT3A binding at *SEMA3A* in response to stilbenoids was confirmed by chromatin immunoprecipitation (Figure 4B). Enrichment of active histone mark and reduction of repressive histone mark further illustrated a transcriptionally active chromatin state at *SEMA3A* (Figure 4C and 4D). *DNMT3A* depletion produced similar effects to those observed after treatment with the compounds demonstrating the involvement of this methylating enzyme in the epigenetic regulation of *SEMA3A* (Figure 4G and 4H). Findings from the *DNMT3A* knockdown experiment provide additional support for DNMT3A as a key protein playing a role in epigenetic activation of *SEMA3A* upon exposure to stilbenoids.

Using TransFac, we predicted NF1C as a candidate transcription factor that binds to regions hypomethylated in response to stilbenoids, including a promoter region of *SEMA3A*. This binding was confirmed experimentally indicating that NF1C is associated with transcriptionally active status of *SEMA3A* after stilbenoid treatment (Figure 5A). Finally, we propose SALL3 as an upstream regulator of loci-specific DNA hypomethylation observed upon exposure to stilbenoids (Figure 5D). SALL3 was previously shown to directly inhibit DNMT3A binding to promote DNA hypomethylation [28]. We observed an increase in *SALL3* expression in response to stilbenoids

(Figure 5C), which may contribute to sequestration of DNMT3A to result in DNA hypomethylation at *SEMA3A* promoter (Figure 5D).

It appears that the epigenetic regulation of *SEMA3A* where DNMT3A is a key mechanistic player is not common to polyphenols as a class of bioactive antioxidant compounds. We tested expression of *SEMA3A*, *DNMT3A*, *NF1C*, and *SALL3* in MCF10CA1a breast cancer cells exposed for 9 days to IC50 concentrations of epigallocatechin gallate (EGCG, green tea polyphenol), genistein (GEN, soy polyphenol), and chlorogenic acids (CGA, coffee polyphenol) (Supplementary Figure S2). GEN and CGA up-regulated *SEMA3A* with concomitant increase in *NF1C* mRNA level (Supplementary Figure S2). Interestingly, none of the compounds decreased expression of *DNMT3A* or increased expression of *SALL3* (Supplementary Figure S2). This finding implies that they do not act through DNMT3A-mediated mechanism to activate *SEMA3A*. This observation remains to be elucidated in future studies.

The proposed series of events may comprise an anti-cancer mechanism prompted by treatment with RSV or PTS. Our findings propose several proteins such as DNMT3A, NF1C and SALL3 as key players in the effects on DNA methylation within potential tumor suppressor genes upon stilbenoid treatment with a goal to use this mechanistic knowledge to implement these compounds into cancer prevention and support of anti-cancer therapies. Importantly, the present study along with our earlier reports indicate that these bioactive compounds exert bidirectional effects on DNA methylation in cancer cells without affecting normal cells which constitutes advantages over standard epigenetic therapies [21, 22, 25, 54].

ACKNOWLEDGEMENTS

This research was supported by the University of British Columbia VP Academic (#10R76632) Award granted to B.S. MCF10CA1h and MCF10CA1a breast cancer cell lines were a kind gift from Dr. Dorothy Teegarden (Department of Nutrition Science, Purdue University, IN, USA).

The Authors declare no conflict of interest.

REFERENCES

[1] Siegel, R. L., Miller, K. D., Jemal, A., Cancer statistics, 2015. *CA: a cancer journal for clinicians* 2015, *65*, 5-29.
[2] Ly, D., Forman, D., Ferlay, J., Brinton, L. A., Cook, M. B., An international comparison of male and female breast cancer incidence rates. *International journal of cancer. Journal international du cancer* 2013, *132*, 1918-1926.
[3] Toska, E., Osmanbeyoglu, H. U., Castel, P., Chan, C., Hendrickson, R. C., Elkabets, M., Dickler, M. N., Scaltriti, M., Leslie, C. S., Armstrong, S. A., Baselga, J., PI3K pathway regulates ER-dependent transcription in breast cancer through the epigenetic regulator KMT2D. *Science* 2017, *355*, 1324-1330.
[4] Jones, P. A., Issa, J. P., Baylin, S., Targeting the cancer epigenome for therapy. *Nature reviews. Genetics* 2016, *17*, 630-641.
[5] Stefanska, B., Huang, J., Bhattacharyya, B., Suderman, M., Hallett, M., Han, Z. G., Szyf, M., Definition of the landscape of promoter DNA hypomethylation in liver cancer. *Cancer research* 2011, *71*, 5891-5903.
[6] Stefanska, B., Bouzelmat, A., Huang, J., Suderman, M., Hallett, M., Han, Z. G., Al-Mahtab, M., Akbar, S. M., Khan, W. A., Raqib, R., Szyf, M., Discovery and Validation of DNA Hypomethylation Biomarkers for Liver Cancer Using HRM-Specific Probes. *PloS one* 2013, *8*, e68439.
[7] Stefanska, B., Suderman, M., Machnes, Z., Bhattacharyya, B., Hallett, M., Szyf, M., Transcription onset of genes critical in liver carcinogenesis is epigenetically regulated by methylated DNA binding protein MBD2. *Carcinogenesis* 2013.
[8] Mayol, G., Martin-Subero, J. I., Rios, J., Queiros, A., Kulis, M., Sunol, M., Esteller, M., Gomez, S., Garcia, I., de Torres, C., Rodriguez, E., Galvan, P., Mora, J., Lavarino, C., DNA hypomethylation affects cancer-related biological functions and genes relevant in neuroblastoma pathogenesis. *PloS one* 2012, *7*, e48401.
[9] Shao, C., Sun, W., Tan, M., Glazer, C. A., Bhan, S., Zhong, X., Fakhry, C., Sharma, R., Westra, W. H., Hoque, M. O., Moskaluk, C. A., Sidransky, D., Califano, J. A., Ha, P. K., Integrated, genome-wide screening for hypomethylated oncogenes in salivary gland adenoid cystic carcinoma. *Clinical cancer research : an official journal of the American Association for Cancer Research* 2011, *17*, 4320-4330.

[10] Stefanska, B., Cheishvili, D., Suderman, M., Arakelian, A., Huang, J., Hallett, M., Han, Z. G., Al-Mahtab, M., Akbar, S. M., Khan, W. A., Raqib, R., Tanvir, I., Khan, H. A., Rabbani, S. A., Szyf, M., Genome-wide study of hypomethylated and induced genes in liver cancer patients unravels novel anticancer targets. *Clinical cancer research : an official journal of the American Association for Cancer Research* 2014.
[11] Rao, X., Evans, J., Chae, H., Pilrose, J., Kim, S., Yan, P., Huang, R. L., Lai, H. C., Lin, H., Liu, Y., Miller, D., Rhee, J. K., Huang, Y. W., Gu, F., Gray, J. W., Huang, T. M., Nephew, K. P., CpG island shore methylation regulates caveolin-1 expression in breast cancer. *Oncogene* 2013, *32*, 4519-4528.
[12] Vizoso, M., Ferreira, H. J., Lopez-Serra, P., Carmona, F. J., Martinez-Cardus, A., Girotti, M. R., Villanueva, A., Guil, S., Moutinho, C., Liz, J., Portela, A., Heyn, H., Moran, S., Vidal, A., Martinez-Iniesta, M., Manzano, J. L., Fernandez-Figueras, M. T., Elez, E., Munoz-Couselo, E., Botella-Estrada, R., Berrocal, A., Ponten, F., Oord, J. V., Gallagher, W. M., Frederick, D. T., Flaherty, K. T., McDermott, U., Lorigan, P., Marais, R., Esteller, M., Epigenetic activation of a cryptic TBC1D16 transcript enhances melanoma progression by targeting EGFR. *Nature medicine* 2015.
[13] Carter, L. G., D'Orazio, J. A., Pearson, K. J., Resveratrol and cancer: focus on in vivo evidence. *Endocrine-related cancer* 2014, *21*, R209-225.
[14] Wang, Y. P., Cheng, M. L., Zhang, B. F., Mu, M., Wu, J., Effects of blueberry on hepatic fibrosis and transcription factor Nrf2 in rats. *World journal of gastroenterology : WJG* 2010, *16*, 2657-2663.
[15] Jeyabalan, J., Aqil, F., Munagala, R., Annamalai, L., Vadhanam, M. V., Gupta, R. C., Chemopreventive and Therapeutic Activity of Dietary Blueberry against Estrogen-Mediated Breast Cancer. *Journal of agricultural and food chemistry* 2014.
[16] Jeyabalan, J., Aqil, F., Munagala, R., Annamalai, L., Vadhanam, M. V., Gupta, R. C., Chemopreventive and therapeutic activity of dietary blueberry against estrogen-mediated breast cancer. *Journal of agricultural and food chemistry* 2014, *62*, 3963-3971.
[17] McCormack, D., McFadden, D., Pterostilbene and cancer: current review. *The Journal of surgical research* 2012, *173*, e53-61.
[18] Wen, W., Lowe, G., Roberts, C. M., Finlay, J., Han, E. S., Glackin, C. A., Dellinger, T. H., Pterostilbene, a natural phenolic compound, synergizes the antineoplastic effects of megestrol acetate in endometrial cancer. *Scientific reports* 2017, *7*, 12754.
[19] Bishayee, A., Politis, T., Darvesh, A. S., Resveratrol in the chemoprevention and treatment of hepatocellular carcinoma. *Cancer treatment reviews* 2010, *36*, 43-53.
[20] Fang, M. Z., Chen, D., Sun, Y., Jin, Z., Christman, J. K., Yang, C. S., Reversal of hypermethylation and reactivation of p16INK4a, RARbeta, and MGMT genes by genistein and other isoflavones from soy. *Clinical cancer research : an official journal of the American Association for Cancer Research* 2005, *11*, 7033-7041.
[21] Stefanska, B., Rudnicka, K., Bednarek, A., Fabianowska-Majewska, K., Hypomethylation and induction of retinoic acid receptor beta 2 by concurrent action of adenosine analogues and natural compounds in breast cancer cells. *European journal of pharmacology* 2010, *638*, 47-53.
[22] Stefanska, B., Salame, P., Bednarek, A., Fabianowska-Majewska, K., Comparative effects of retinoic acid, vitamin D and resveratrol alone and in combination with adenosine analogues on methylation and expression of phosphatase and tensin homologue tumour suppressor gene in breast cancer cells. *The British journal of nutrition* 2012, *107*, 781-790.

[23] Lee, W. J., Zhu, B. T., Inhibition of DNA methylation by caffeic acid and chlorogenic acid, two common catechol-containing coffee polyphenols. *Carcinogenesis* 2006, *27*, 269-277.
[24] Papoutsis, A. J., Borg, J. L., Selmin, O. I., Romagnolo, D. F., BRCA-1 promoter hypermethylation and silencing induced by the aromatic hydrocarbon receptor-ligand TCDD are prevented by resveratrol in MCF-7 cells. *The Journal of nutritional biochemistry* 2012, *23*, 1324-1332.
[25] Lubecka, K., Kurzava, L., Flower, K., Buvala, H., Zhang, H., Teegarden, D., Camarillo, I., Suderman, M., Kuang, S., Andrisani, O., Flanagan, J. M., Stefanska, B., Stilbenoids remodel the DNA methylation patterns in breast cancer cells and inhibit oncogenic NOTCH signaling through epigenetic regulation of MAML2 transcriptional activity. *Carcinogenesis* 2016, *37*, 656-668.
[26] Mishra, R., Thorat, D., Soundararajan, G., Pradhan, S. J., Chakraborty, G., Lohite, K., Karnik, S., Kundu, G. C., Semaphorin 3A upregulates FOXO 3a-dependent MelCAM expression leading to attenuation of breast tumor growth and angiogenesis. *Oncogene* 2015, *34*, 1584-1595.
[27] Wallerius, M., Wallmann, T., Bartish, M., Ostling, J., Mezheyeuski, A., Tobin, N. P., Nygren, E., Pangigadde, P., Pellegrini, P., Squadrito, M. L., Ponten, F., Hartman, J., Bergh, J., De Milito, A., De Palma, M., Ostman, A., Andersson, J., Rolny, C., Guidance Molecule SEMA3A Restricts Tumor Growth by Differentially Regulating the Proliferation of Tumor-Associated Macrophages. *Cancer research* 2016, *76*, 3166-3178.
[28] Shikauchi, Y., Saiura, A., Kubo, T., Niwa, Y., Yamamoto, J., Murase, Y., Yoshikawa, H., SALL3 interacts with DNMT3A and shows the ability to inhibit CpG island methylation in hepatocellular carcinoma. *Molecular and cellular biology* 2009, *29*, 1944-1958.
[29] Colella, S., Shen, L., Baggerly, K. A., Issa, J. P., Krahe, R., Sensitive and quantitative universal Pyrosequencing methylation analysis of CpG sites. *BioTechniques* 2003, *35*, 146-150.
[30] Tost, J., Gut, I. G., DNA methylation analysis by pyrosequencing. *Nature protocols* 2007, *2*, 2265-2275.
[31] Pfaffl, M. W., Horgan, G. W., Dempfle, L., Relative expression software tool (REST) for group-wise comparison and statistical analysis of relative expression results in real-time PCR. *Nucleic acids research* 2002, *30*, e36.
[32] Taylor, S. C., Nadeau, K., Abbasi, M., Lachance, C., Nguyen, M., Fenrich, J., The Ultimate qPCR Experiment: Producing Publication Quality, Reproducible Data the First Time. *Trends in biotechnology* 2019.
[33] Brown, S. E., Suderman, M. J., Hallett, M., Szyf, M., DNA demethylation induced by the methyl-CpG-binding domain protein MBD3. *Gene* 2008, *420*, 99-106.
[34] Peng, G. H., Chen, S., Double chromatin immunoprecipitation: analysis of target co-occupancy of retinal transcription factors. *Methods in molecular biology* 2013, *935*, 311-328.
[35] Wilhelm-Benartzi, C. S., Koestler, D. C., Karagas, M. R., Flanagan, J. M., Christensen, B. C., Kelsey, K. T., Marsit, C. J., Houseman, E. A., Brown, R., Review of processing and analysis methods for DNA methylation array data. *British journal of cancer* 2013, *109*, 1394-1402.
[36] Chen, M., Zhu, N., Liu, X., Laurent, B., Tang, Z., Eng, R., Shi, Y., Armstrong, S. A., Roeder, R. G., JMJD1C is required for the survival of acute myeloid leukemia by functioning as a coactivator for key transcription factors. *Genes & development* 2015, *29*, 2123-2139.
[37] Sengelaub, C. A., Navrazhina, K., Ross, J. B., Halberg, N., Tavazoie, S. F., PTPRN2 and PLCbeta1 promote metastatic breast cancer cell migration through PI(4,5)P2-dependent actin remodeling. *The EMBO journal* 2016, *35*, 62-76.

[38] Chen, D., Sun, Y., Wei, Y., Zhang, P., Rezaeian, A. H., Teruya-Feldstein, J., Gupta, S., Liang, H., Lin, H. K., Hung, M. C., Ma, L., LIFR is a breast cancer metastasis suppressor upstream of the Hippo-YAP pathway and a prognostic marker. *Nature medicine* 2012, *18*, 1511-1517.
[39] Kamal, M., Holliday, D. L., Morrison, E. E., Speirs, V., Toomes, C., Bell, S. M., Loss of CSMD1 expression disrupts mammary duct formation while enhancing proliferation, migration and invasion. *Oncology reports* 2017, *38*, 283-292.
[40] Maiga, A., Lemieux, S., Pabst, C., Lavallee, V. P., Bouvier, M., Sauvageau, G., Hebert, J., Transcriptome analysis of G protein-coupled receptors in distinct genetic subgroups of acute myeloid leukemia: identification of potential disease-specific targets. *Blood cancer journal* 2016, *6*, e431.
[41] Jiang, X., Yu, Y., Yang, H. W., Agar, N. Y., Frado, L., Johnson, M. D., The imprinted gene PEG3 inhibits Wnt signaling and regulates glioma growth. *The Journal of biological chemistry* 2010, *285*, 8472-8480.
[42] Liu, Y., Amin, E. B., Mayo, M. W., Chudgar, N. P., Bucciarelli, P. R., Kadota, K., Adusumilli, P. S., Jones, D. R., CK2alpha' Drives Lung Cancer Metastasis by Targeting BRMS1 Nuclear Export and Degradation. *Cancer research* 2016, *76*, 2675-2686.
[43] Tang, N., Ma, L., Lin, X. Y., Zhang, Y., Yang, D. L., Wang, E. H., Qiu, X. S., Expression of PHF20 protein contributes to good prognosis of NSCLC and is associated with Bax expression. *International journal of clinical and experimental pathology* 2015, *8*, 12198-12206.
[44] Rabello Ddo, A., de Moura, C. A., de Andrade, R. V., Motoyama, A. B., Silva, F. P., Altered expression of MLL methyltransferase family genes in breast cancer. *International journal of oncology* 2013, *43*, 653-660.
[45] Herman, J. G., Meadows, G. G., Increased class 3 semaphorin expression modulates the invasive and adhesive properties of prostate cancer cells. *International journal of oncology* 2007, *30*, 1231-1238.
[46] Dai, Y., Wang, M., Wu, H., Xiao, M., Liu, H., Zhang, D., Loss of FOXN3 in colon cancer activates beta-catenin/TCF signaling and promotes the growth and migration of cancer cells. *Oncotarget* 2017, *8*, 9783-9793.
[47] Escudero-Esparza, A., Bartoschek, M., Gialeli, C., Okroj, M., Owen, S., Jirstrom, K., Orimo, A., Jiang, W. G., Pietras, K., Blom, A. M., Complement inhibitor CSMD1 acts as tumor suppressor in human breast cancer. *Oncotarget* 2016, *7*, 76920-76933.
[48] Xu, T., Park, S. S., Giaimo, B. D., Hall, D., Ferrante, F., Ho, D. M., Hori, K., Anhezini, L., Ertl, I., Bartkuhn, M., Zhang, H., Milon, E., Ha, K., Conlon, K. P., Kuick, R., Govindarajoo, B., Zhang, Y., Sun, Y., Dou, Y., Basrur, V., Elenitoba-Johnson, K. S., Nesvizhskii, A. I., Ceron, J., Lee, C. Y., Borggrefe, T., Kovall, R. A., Rual, J. F., RBPJ/CBF1 interacts with L3MBTL3/MBT1 to promote repression of Notch signaling via histone demethylase KDM1A/LSD1. *The EMBO journal* 2017, *36*, 3232-3249.
[49] Yin, Y., Morgunova, E., Jolma, A., Kaasinen, E., Sahu, B., Khund-Sayeed, S., Das, P. K., Kivioja, T., Dave, K., Zhong, F., Nitta, K. R., Taipale, M., Popov, A., Ginno, P. A., Domcke, S., Yan, J., Schubeler, D., Vinson, C., Taipale, J., Impact of cytosine methylation on DNA binding specificities of human transcription factors. *Science* 2017, *356*.
[50] Fane, M., Harris, L., Smith, A. G., Piper, M., Nuclear factor one transcription factors as epigenetic regulators in cancer. *International journal of cancer. Journal international du cancer* 2017, *140*, 2634-2641.

[51] Lee, H. K., Lee, D. S., Park, J. C., Nuclear factor I-C regulates E-cadherin via control of KLF4 in breast cancer. *BMC cancer* 2015, *15*, 113.
[52] Yun, H., Damm, F., Yap, D., Schwarzer, A., Chaturvedi, A., Jyotsana, N., Lubbert, M., Bullinger, L., Dohner, K., Geffers, R., Aparicio, S., Humphries, R. K., Ganser, A., Heuser, M., Impact of MLL5 expression on decitabine efficacy and DNA methylation in acute myeloid leukemia. *Haematologica* 2014, *99*, 1456-1464.
[53] Qin, T., Castoro, R., El Ahdab, S., Jelinek, J., Wang, X., Si, J., Shu, J., He, R., Zhang, N., Chung, W., Kantarjian, H. M., Issa, J. P., Mechanisms of resistance to decitabine in the myelodysplastic syndrome. *PloS one* 2011, *6*, e23372.
[54] Link, A., Balaguer, F., Shen, Y., Lozano, J. J., Leung, H. C., Boland, C. R., Goel, A., Curcumin modulates DNA methylation in colorectal cancer cells. *PloS one* 2013, *8*, e57709.
[55] Lou, X. D., Wang, H. D., Xia, S. J., Skog, S., Sun, J., Effects of resveratrol on the expression and DNA methylation of cytokine genes in diabetic rat aortas. *Archivum immunologiae et therapiae experimentalis* 2014, *62*, 329-340.
[56] Gracia, A., Elcoroaristizabal, X., Fernandez-Quintela, A., Miranda, J., Bediaga, N. G., M, M. d. P., Rimando, A. M., Portillo, M. P., Fatty acid synthase methylation levels in adipose tissue: effects of an obesogenic diet and phenol compounds. *Genes & nutrition* 2014, *9*, 411.
[57] Shiiba, M., Nomura, H., Shinozuka, K., Saito, K., Kouzu, Y., Kasamatsu, A., Sakamoto, Y., Murano, A., Ono, K., Ogawara, K., Uzawa, K., Tanzawa, H., Down-regulated expression of SERPIN genes located on chromosome 18q21 in oral squamous cell carcinomas. *Oncology reports* 2010, *24*, 241-249.
[58] Li, X., Wang, J., Zhang, C., Lin, C., Zhang, J., Zhang, W., Zhang, W., Lu, Y., Zheng, L., Li, X., Circular RNA circITGA7 inhibits colorectal cancer growth and metastasis by modulating the Ras pathway and upregulating transcription of its host gene ITGA7. *The Journal of pathology* 2018, *246*, 166-179.
[59] Bhandari, A., Xia, E., Zhou, Y., Guan, Y., Xiang, J., Kong, L., Wang, Y., Yang, F., Wang, O., Zhang, X., ITGA7 functions as a tumor suppressor and regulates migration and invasion in breast cancer. *Cancer management and research* 2018, *10*, 969-976.
[60] Yokoi, A., Yoshioka, Y., Yamamoto, Y., Ishikawa, M., Ikeda, S. I., Kato, T., Kiyono, T., Takeshita, F., Kajiyama, H., Kikkawa, F., Ochiya, T., Malignant extracellular vesicles carrying MMP1 mRNA facilitate peritoneal dissemination in ovarian cancer. *Nature communications* 2017, *8*, 14470.
[61] Shen, C. J., Kuo, Y. L., Chen, C. C., Chen, M. J., Cheng, Y. M., MMP1 expression is activated by Slug and enhances multi-drug resistance (MDR) in breast cancer. *PloS one* 2017, *12*, e0174487.
[62] Jilaveanu, L. B., Parisi, F., Barr, M. L., Zito, C. R., Cruz-Munoz, W., Kerbel, R. S., Rimm, D. L., Bosenberg, M. W., Halaban, R., Kluger, Y., Kluger, H. M., PLEKHA5 as a Biomarker and Potential Mediator of Melanoma Brain Metastasis. *Clinical cancer research : an official journal of the American Association for Cancer Research* 2015, *21*, 2138-2147.
[63] Wu, W. F., Maneix, L., Insunza, J., Nalvarte, I., Antonson, P., Kere, J., Yu, N. Y., Tohonen, V., Katayama, S., Einarsdottir, E., Krjutskov, K., Dai, Y. B., Huang, B., Su, W., Warner, M., Gustafsson, J. A., Estrogen receptor beta, a regulator of androgen receptor signaling in the mouse ventral prostate. *Proceedings of the National Academy of Sciences of the United States of America* 2017, *114*, E3816-E3822.

[64] Dellinger, R. W., Garcia, A. M., Meyskens, F. L., Jr., Differences in the glucuronidation of resveratrol and pterostilbene: altered enzyme specificity and potential gender differences. *Drug metabolism and pharmacokinetics* 2014, *29*, 112-119.

FIGURE LEGENDS

Figure 1. Landscape of changes in the DNA methylation patterns in breast cancer cells in response to resveratrol (RSV). (A) A comparison of the number of differentially methylated CpG sites with statistically significant difference of at least 0.05 between RSV-treated and control cells (i.e., delta beta) on day 4 and day 9 exposure to 15μM RSV in MCF10CA1h lowly invasive breast cancer cells, as determined by Illumina 450K microarray ($P < 0.05$, limma *t*-test). (B) Magnitude of methylation difference between RSV-treated and control cells at genes and gene families differentially methylated as indicated by the microarray data upon 4-day and 9-day exposure of MCF10CA1h breast cancer cells. (C) A comparison of the number of differentially methylated CpG sites with statistically significant difference of at least 0.05 between RSV-treated and control cells on day 9 exposure to 15μM RSV in MCF10CA1h lowly invasive and MCF10CA1a highly invasive breast cancer cells, as determined by Illumina 450K microarray ($P < 0.05$, limma *t*-test). (D) Magnitude of overall methylation changes upon treatment of MCF10CA1h and MCF10CA1a breast cancer cells with RSV. (E) Venn diagram for genes containing CpG sites hypomethylated in response to RSV in MCF10CA1h and MCF10CA1a breast cancer cells, showing overlap between both cell lines. (F,G) Basal levels of methylation of "hypomethylated RSV targets" as determined by the genome-wide microarray data in untreated MCF10A mammary epithelial cells, MCF10CA1h lowly invasive and MCF10CA1a highly invasive breast cancer cells (F), as well as in breast cancer cells exposed to 15μM RSV for 9 days (G). The basal level of methylation at CpG loci commonly hypomethylated in MCF10CA1h lowly invasive and MCF10CA1a highly invasive

breast cancer cells upon 9-day RSV treatment is compared to the methylation levels at these loci in MCF10A cells. (H,I) Functional analyses using GO, KEGG and DAVID knowledgebase indicate biological functions (H) and signaling pathways (I) associated with genes corresponding to CpG sites hypomethylated in response to RSV in both MCF10CA1h and MCF10CA1a breast cancer cells ("hypomethylated RSV targets").

Figure 2. Quantitative analysis of methylation state of the selected genes, *SEMA3A*, *UACA*, *FAM49A, TMEM91,* and *EPN2,* which contain CpG loci highly hypomethylated in invasive MCF10CA1a breast cancer cells exposed to resveratrol (RSV) based on the Illumina 450K microarray. Using Illumina 450K microarray, the DNA methylation landscape was determined in lowly and highly invasive breast cancer cells exposed to 15 μM RSV for 9 days. Based on the microarray data, 5 hypomethylated CpG sites corresponding to 5 genes (probes) were chosen for validation of the methylation difference by pyrosequencing. The difference in DNA methylation, statistical significance, location of the CpG site in gene regulatory region, consistency of the change between the cell lines, and the function of a corresponding gene as a potential tumor suppressor gene were taken into account in the selection. (A) Magnitude of methylation difference between RSV-treated and control cells at CpG loci corresponding to 10 genes that are highly hypomethylated in response to RSV in invasive MCF10CA1a breast cancer cells upon 9-day treatment, as indicated by the microarray data. (B) Right panel shows the average methylation state at single CpG sites within the selected probes in control MCF10CA1a cells (treated with ethanol as a vehicle control) and MCF10CA1a cells exposed to 15μM RSV for 9 days. Each region encompasses a differentially methylated CpG site covered on Illumina 450K microarray (marked in square) along with neighboring CpG loci. Gene maps in the left panel show the exact position

of the tested CpG sites relative to transcription start site (TSS). The tested region is shaded and pyrosequenced CpG sites are circled and numbered. The putative transcription factor binding sites are indicated as predicted by TransFac. All results represent mean ± SD of three independent experiments; ***$P < 0.001$, **$P < 0.01$, *$P < 0.05$.

Figure 3. *SEMA3A* tumor suppressor gene is hypomethylated and reactivated upon treatment of highly invasive MCF10CA1a breast cancer cells with pterostilbene (PTS). (A) *SEMA3A* expression in normal and cancer tissues based on microarray data from Oncomine database. Expression values are presented as $\log_2$-transformed median centered per array, and SD-normalized to 1 per array. (B) *SEMA3A* methylation state within three CpG sites (X axis) expressed as beta value in normal and cancer tissues (Y axis), based on Illumina human methylation microarray data from publicly available datasets of breast cancer patients (TCGA). Beta value represents a methylation score for a given CpG site according to the fluorescent intensity ratio detected on the microarray with any values between 0 (unmethylated) and 1 (completely methylated). The chart confirms hypermethylation of *SEMA3A* promoter region in tumors at the same CpG locus as the site affected by RSV (the locus marked in square). (C) Hypomethylation of *SEMA3A* promoter upon 9-day exposure to 7μM PTS in MCF10CA1a breast cancer cells, as measured by pyrosequencing. (D) Increased expression of *SEMA3A* upon 9-day exposure to 15μM RSV or 7μM PTS in MCF10CA1a breast cancer cells, as measured by qPCR. (E) Hypomethylation and increased expression of *SEMA3A* in response to 9-day exposure to 15μM RSV in lowly invasive MCF10CA1h breast cancer cells, as measured by pyrosequencing and qPCR, respectively. All results represent mean ± SD of three independent experiments; ***$P < 0.001$, **$P < 0.01$, *$P < 0.05$.

Figure 4. Binding of DNMT3A and modifications of histone tails within *SEMA3A* promoter in breast cancer cells in response to resveratrol (RSV) or pterostilbene (PTS): a key role of DNMT3A. (A) Expression of *DNMT3A* upon 9-day exposure to 15 µM RSV or 7 µM PTS in MCF10CA1a breast cancer cells, as measured by QPCR. (B) Binding of DNMT3A within the *SEMA3A* promoter in MCF10CA1a cells in response to 9-day treatment with 15 µM RSV or 7 µM PTS, as assessed by qChIP and expressed as a percentage of the binding level in control cells. (C,D) Enrichment of histone H3 acetylation at lysine 9 (H3K9ac, activating mark) (C) and histone H3 trimethylation at lysine 27 (H3K27me3, repressive mark) (D) within the *SEMA3A* promoter in MCF10CA1a cells in response to 9-day treatment with 15 µM RSV or 7 µM PTS, as assessed by qChIP and expressed as a percentage of the binding level in control cells. (E) Effect on MCF10CA1a cell growth after first (day 3), second (day 6) and third (day 9) transfection with siCtrl or siDNMT3A #1-4. (F) *DNMT3A* expression quantified by qPCR after third transfection with siCtrl or siDNMT3A #1-4. (G) Increased *SEMA3A* expression quantified by qPCR after third transfection with siDNMT3A #1 or siDNMT3A #3 compared to siCtrl. (H) Hypomethylation of *SEMA3A* quantified by pyrosequencing after third transfection with siDNMT3A #1 or siDNMT3A #3 compared to siCtrl. All results represent mean ± SD of three independent experiments; ***$P < 0.001$, **$P < 0.01$, *$P < 0.05$.

Figure 5. Occupancy of transcription factor NF1C within *SEMA3A* promoter and potential role for SALL3 in breast cancer cells in response to resveratrol (RSV) or pterostilbene (PTS). (A) Binding of NF1C within the *SEMA3A* promoter in MCF10CA1a cells in response to 9-day treatment with 15 µM RSV or 7 µM PTS as assessed by qChIP and expressed as a percentage of

the binding level in control cells. (B) Expression of *NF1C* upon 9-day exposure to 15 μM RSV or 7 μM PTS in MCF10CA1a breast cancer cells, as measured by qPCR. (C) *SALL3* expression quantified by qPCR in MCF10CA1a cells in response to 9-day treatment with 15 μM RSV or 7 μM PTS. (D) Schematic of proposed mechanism of stilbenoid-mediated epigenetic reactivation of *SEMA3A* involving direct inhibition of DNMT3A by SALL3 to impose DNA hypomethylation and allow NF1C to bind at the *SEMA3A* promoter and drive gene transcription. All results represent mean ± SD of three independent experiments; ***$P < 0.001$, **$P < 0.01$, *$P < 0.05$.

Table 1. A list of CpG loci highly hypomethylated in invasive MCF10CA1a cells in response to 9-day exposure to 15μM resveratrol (RSV), as measured by Illumina Infinium Human Methylation 450K BeadChip microarray.

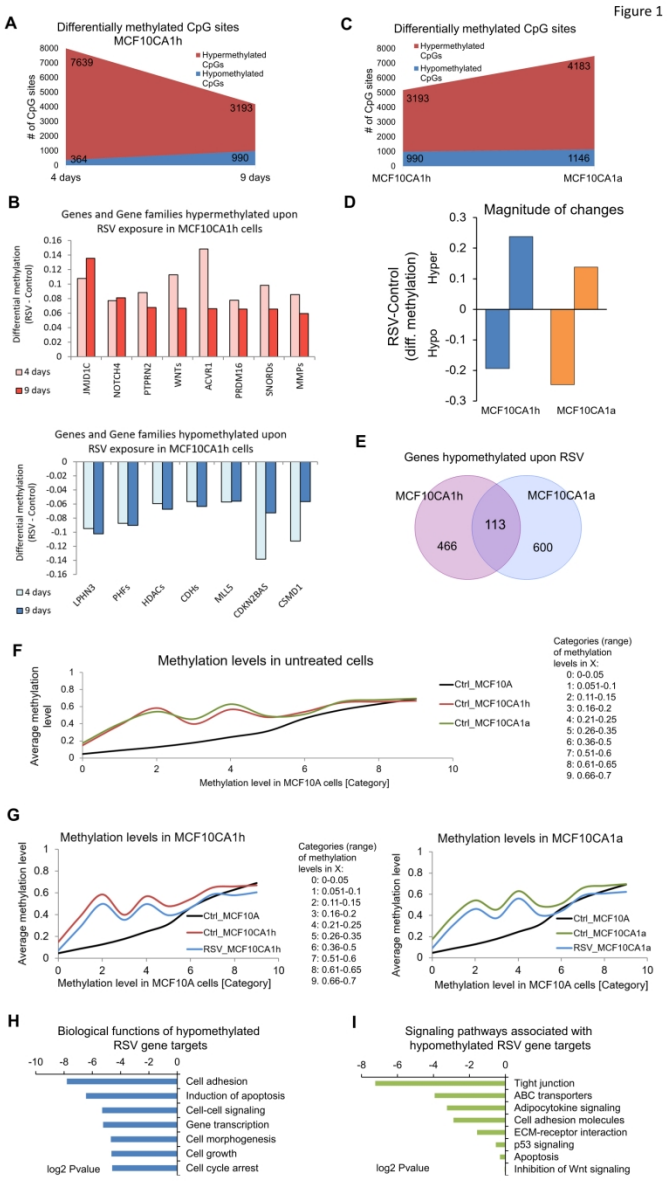

Figure 1. Landscape of changes in the DNA methylation patterns in breast cancer cells in response to resveratrol (RSV). (A) A comparison of the number of differentially methylated CpG sites with statistically significant difference of at least 0.05 between RSV-treated and control cells (i.e., delta beta) on day 4 and day 9 exposure to 15μM RSV in MCF10CA1h lowly invasive breast cancer cells, as determined by Illumina 450K microarray ($P < 0.05$, limma t-test). (B) Magnitude of methylation difference between RSV-treated and control cells at genes and gene families differentially methylated as indicated by the microarray data upon 4-day and 9-day exposure of MCF10CA1h breast cancer cells. (C) A comparison of the number of differentially methylated CpG sites with statistically significant difference of at least 0.05 between RSV-treated and control cells on day 9 exposure to 15μM RSV in MCF10CA1h lowly invasive and MCF10CA1a highly invasive breast cancer cells, as determined by Illumina 450K microarray ($P < 0.05$, limma t-test). (D) Magnitude of overall methylation changes upon treatment of MCF10CA1h and MCF10CA1a breast cancer cells with RSV. (E) Venn diagram for genes containing CpG sites hypomethylated in response to RSV in MCF10CA1h and MCF10CA1a breast cancer cells, showing overlap between both cell lines. (F,G) Basal levels

of methylation of "hypomethylated RSV targets" as determined by the genome-wide microarray data in untreated MCF10A mammary epithelial cells, MCF10CA1h lowly invasive and MCF10CA1a highly invasive breast cancer cells (F), as well as in breast cancer cells exposed to 15μM RSV for 9 days (G). The basal level of methylation at CpG loci commonly hypomethylated in MCF10CA1h lowly invasive and MCF10CA1a highly invasive breast cancer cells upon 9-day RSV treatment is compared to the methylation levels at these loci in MCF10A cells. (H,I) Functional analyses using GO, KEGG and DAVID knowledgebase indicate biological functions (H) and signaling pathways (I) associated with genes corresponding to CpG sites hypomethylated in response to RSV in both MCF10CA1h and MCF10CA1a breast cancer cells ("hypomethylated RSV targets").

139x249mm (300 x 300 DPI)

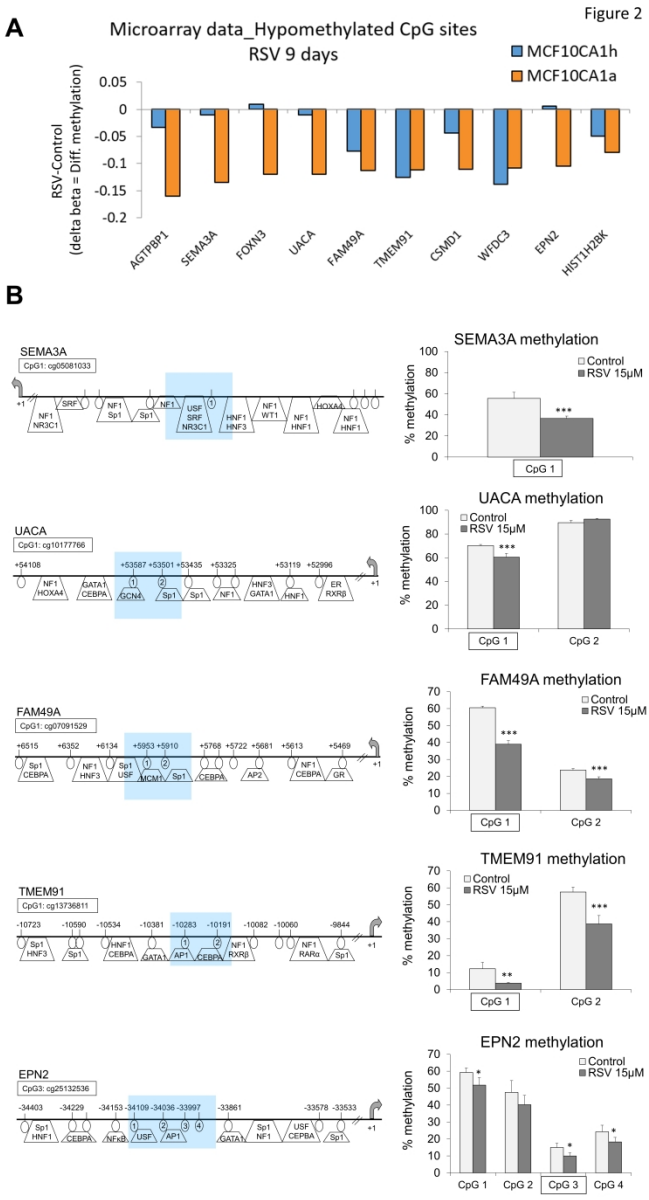

Figure 2. Quantitative analysis of methylation state of the selected genes, SEMA3A, UACA, FAM49A, TMEM91, and EPN2, which contain CpG loci highly hypomethylated in invasive MCF10CA1a breast cancer cells exposed to resveratrol (RSV) based on the Illumina 450K microarray. Using Illumina 450K microarray, the DNA methylation landscape was determined in lowly and highly invasive breast cancer cells exposed to 15 μM RSV for 9 days. Based on the microarray data, 5 hypomethylated CpG sites corresponding to 5 genes (probes) were chosen for validation of the methylation difference by pyrosequencing. The difference in DNA methylation, statistical significance, location of the CpG site in gene regulatory region, consistency of the change between the cell lines, and the function of a corresponding gene as a potential tumor suppressor gene were taken into account in the selection. (A) Magnitude of methylation difference between RSV-treated and control cells at CpG loci corresponding to 10 genes that are highly hypomethylated in response to RSV in invasive MCF10CA1a breast cancer cells upon 9-day treatment, as indicated by the microarray data. (B) Right panel shows the average methylation state at single CpG sites within the selected probes in control MCF10CA1a cells (treated with ethanol as a vehicle control) and MCF10CA1a cells exposed to 15μM RSV for 9 days. Each region encompasses a differentially methylated CpG site covered on Illumina 450K

microarray (marked in square) along with neighboring CpG loci. Gene maps in the left panel show the exact position of the tested CpG sites relative to transcription start site (TSS). The tested region is shaded and pyrosequenced CpG sites are circled and numbered. The putative transcription factor binding sites are indicated as predicted by TransFac. All results represent mean ± SD of three independent experiments; ***P < 0.001, **P < 0.01, *P < 0.05.

360x660mm (300 x 300 DPI)

Figure 3

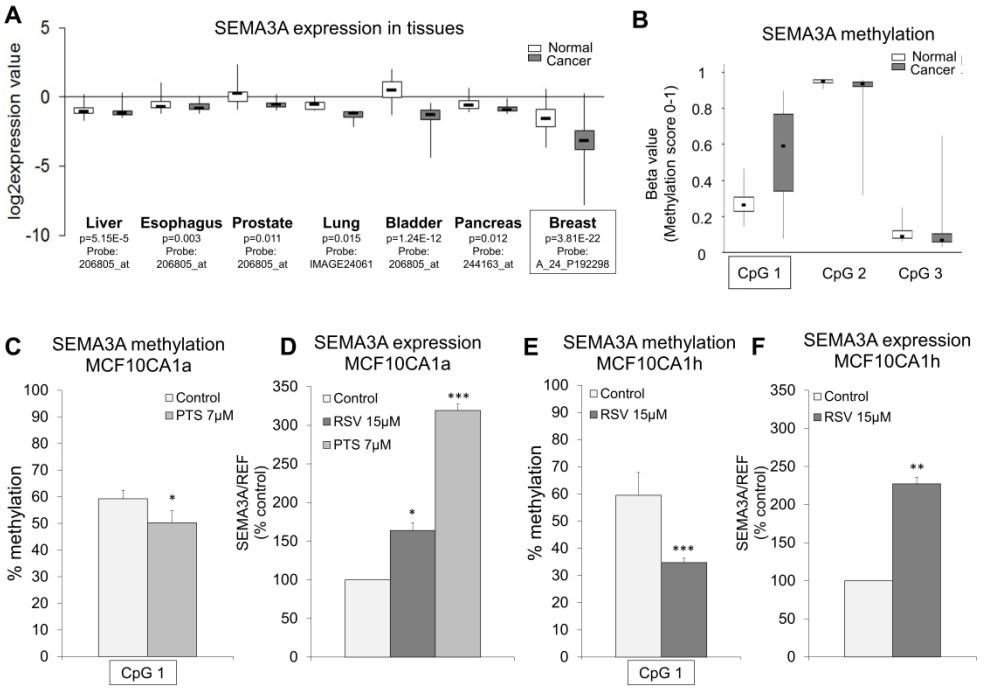

Figure 3. SEMA3A tumor suppressor gene is hypomethylated and reactivated upon treatment of highly invasive MCF10CA1a breast cancer cells with pterostilbene (PTS). (A) SEMA3A expression in normal and cancer tissues based on microarray data from Oncomine database. Expression values are presented as log2-transformed median centered per array, and SD-normalized to 1 per array. (B) SEMA3A methylation state within three CpG sites (X axis) expressed as beta value in normal and cancer tissues (Y axis), based on Illumina human methylation microarray data from publicly available datasets of breast cancer patients (TCGA). Beta value represents a methylation score for a given CpG site according to the fluorescent intensity ratio detected on the microarray with any values between 0 (unmethylated) and 1 (completely methylated). The chart confirms hypermethylation of SEMA3A promoter region in tumors at the same CpG locus as the site affected by RSV (the locus marked in square). (C) Hypomethylation of SEMA3A promoter upon 9-day exposure to 7μM PTS in MCF10CA1a breast cancer cells, as measured by pyrosequencing. (D) Increased expression of SEMA3A upon 9-day exposure to 15μM RSV or 7μM PTS in MCF10CA1a breast cancer cells, as measured by qPCR. (E) Hypomethylation and increased expression of SEMA3A in response to 9-day exposure to 15μM RSV in lowly invasive MCF10CA1h breast cancer cells, as measured by pyrosequencing and qPCR, respectively. All results represent mean ± SD of three independent experiments; ***P < 0.001, **P < 0.01, *P < 0.05.

459x330mm (300 x 300 DPI)

Figure 4

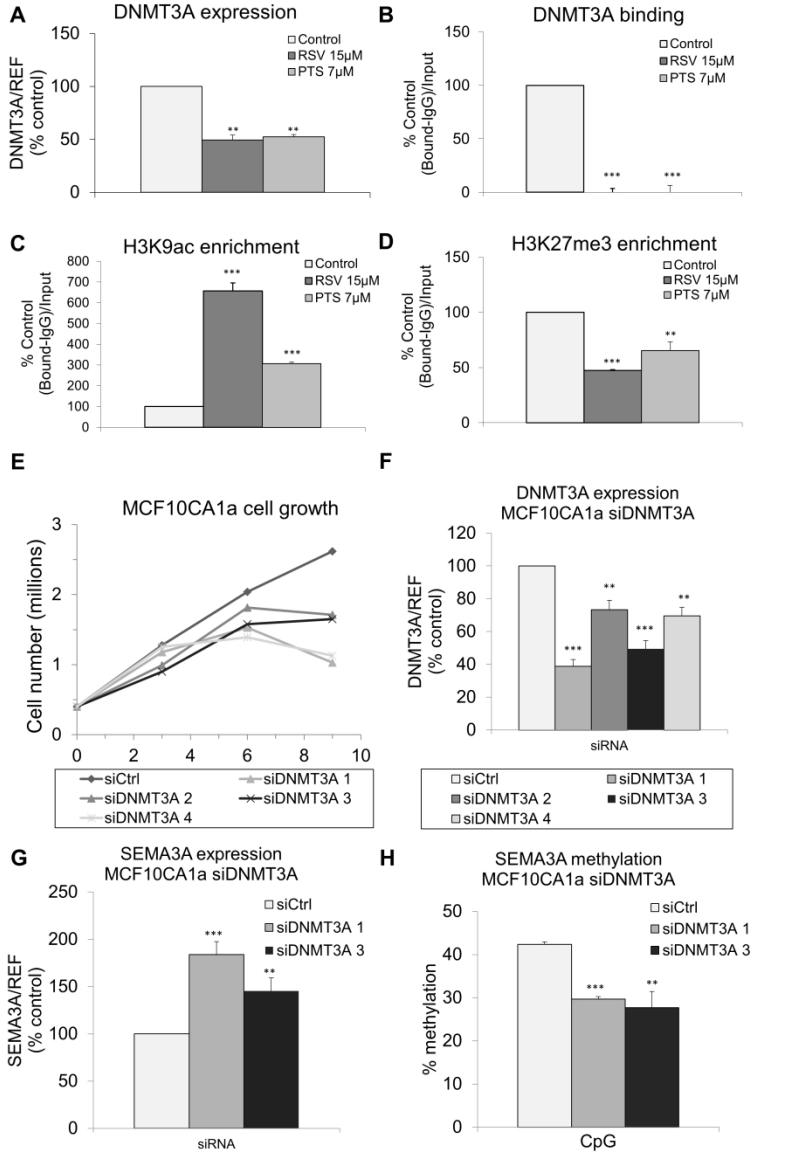

Figure 4. Binding of DNMT3A and modifications of histone tails within SEMA3A promoter in breast cancer cells in response to resveratrol (RSV) or pterostilbene (PTS): a key role of DNMT3A. (A) Expression of DNMT3A upon 9-day exposure to 15 μM RSV or 7 μM PTS in MCF10CA1a breast cancer cells, as measured by QPCR. (B) Binding of DNMT3A within the SEMA3A promoter in MCF10CA1a cells in response to 9-day treatment with 15 μM RSV or 7 μM PTS, as assessed by qChIP and expressed as a percentage of the binding level in control cells. (C,D) Enrichment of histone H3 acetylation at lysine 9 (H3K9ac, activating mark) (C) and histone H3 trimethylation at lysine 27 (H3K27me3, repressive mark) (D) within the SEMA3A promoter in MCF10CA1a cells in response to 9-day treatment with 15 μM RSV or 7 μM PTS, as assessed by qChIP and expressed as a percentage of the binding level in control cells. (E) Effect on MCF10CA1a cell growth after first (day 3), second (day 6) and third (day 9) transfection with siCtrl or siDNMT3A #1-4. (F) DNMT3A expression quantified by qPCR after third transfection with siCtrl or siDNMT3A #1-4. (G) Increased SEMA3A expression quantified by qPCR after third transfection with siDNMT3A #1 or siDNMT3A #3 compared to siCtrl. (H) Hypomethylation of SEMA3A quantified by pyrosequencing after third transfection with siDNMT3A #1 or siDNMT3A #3 compared to siCtrl. All results represent mean ± SD of three independent experiments;

***P < 0.001, **P < 0.01, *P < 0.05.

254x381mm (300 x 300 DPI)

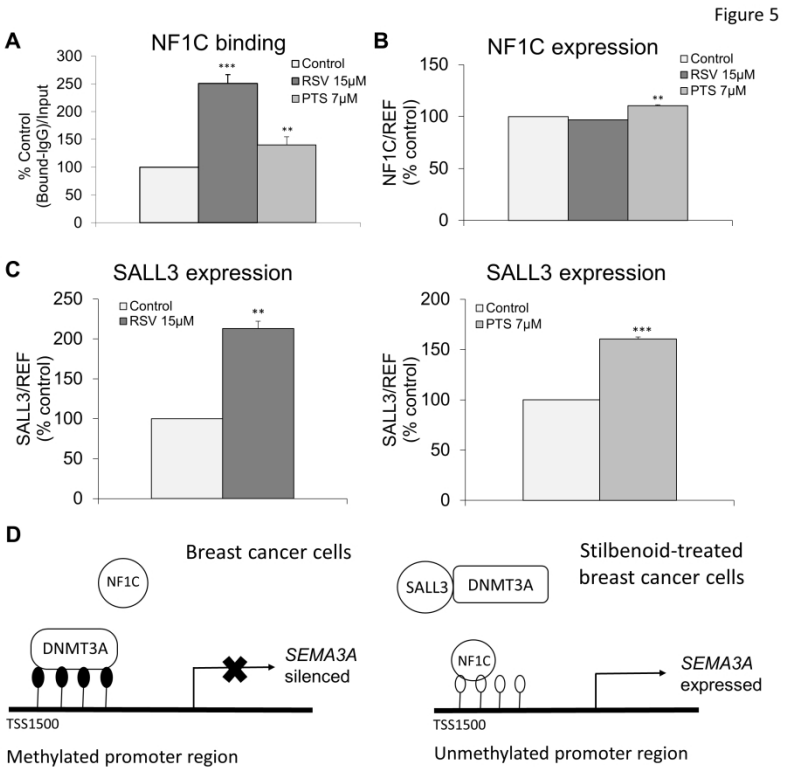

Figure 5. Occupancy of transcription factor NF1C within SEMA3A promoter and potential role for SALL3 in breast cancer cells in response to resveratrol (RSV) or pterostilbene (PTS). (A) Binding of NF1C within the SEMA3A promoter in MCF10CA1a cells in response to 9-day treatment with 15 μM RSV or 7 μM PTS as assessed by qChIP and expressed as a percentage of the binding level in control cells. (B) Expression of NF1C upon 9-day exposure to 15 μM RSV or 7 μM PTS in MCF10CA1a breast cancer cells, as measured by qPCR. (C) SALL3 expression quantified by qPCR in MCF10CA1a cells in response to 9-day treatment with 15 μM RSV or 7 μM PTS. (D) Schematic of proposed mechanism of stilbenoid-mediated epigenetic reactivation of SEMA3A involving direct inhibition of DNMT3A by SALL3 to impose DNA hypomethylation and allow NF1C to bind at the SEMA3A promoter and drive gene transcription. All results represent mean ± SD of three independent experiments; ***P < 0.001, **P < 0.01, *P < 0.05.

254x381mm (300 x 300 DPI)

Table 1. A list of CpG loci highly hypomethylated in invasive MCF10CA1a cells in response to 9-day exposure to 15 μM resveratrol (RSV), as measured by Illumina Infinium Human Methylation 450K BeadChip microarray.

Gene name	CpG #	CpG location	Differential methylation in MCF10CA1h (delta beta)	Differential methylation in MCF10CA1a (delta beta)
AGTPBP1	cg14079243	TSS1500	-0.03	-0.16
SEMA3A	cg05081033	TSS1500	-0.01	-0.14
FOXN3	cg14843872	5'UTR	0.01	-0.12
UACA	cg10177766	Body	-0.01	-0.12
FAM49A	cg07091529	5'UTR	-0.08	-0.11
TMEM91	cg13736811	5'UTR	-0.13	-0.11
CSMD1	cg25114299	Body	-0.04	-0.11
WFDC3	cg07982740	Body	-0.14	-0.11
EPN2	cg25132536	5'UTR	0.01	-0.10
CSMD3	cg00417291	5'UTR	-0.03	-0.10
CDKN2BAS	cg14069088	Body	-0.07	-0.08
HIST1H2BK	cg23155468	3'UTR	-0.05	-0.08
SEMA3D	cg26801812	Body	-0.01	-0.08
HAT1	cg04507121	TSS1500	-0.01	-0.08